FULL PAPER

Core-Brominated Tetraazaperopyrenes as n-Channel Semiconductors for Organic Complementary Circuits on Flexible Substrates

Sonja Geib, Ute Zschieschang, Marcel Gsänger, Matthias Stolte, Frank Würthner, Hubert Wadepohl, Hagen Klauk,* and Lutz H. Gade*

Organic thin-film transistors (TFTs) are prepared by vacuum deposition and solution shearing of 2,9-bis(perfluoroalkyl)-substituted tetraazaperopyrenes (TAPPs) with bromine substituents at the aromatic core. The TAPP derivatives are synthesized by reacting known unsubstituted TAPPs with bromine in fuming sulphuric acid, and their electrochemical properties are studied in detail by cyclic voltammetry and modelled with density functional theory (DFT) methods. Lowest unoccupied molecular orbital (LUMO) energies and electron affinities indicate that the core-brominated TAPPs should exhibit n-channel semiconducting properties. Current-voltage characteristics of the TFTs established electron mobilities of up to $\mu_n = 0.032$ cm^2 V^{-1} s^{-1} for a derivative which was subsequently processed in the fabrication of a complementary ring oscillator on a flexible plastic substrate (PEN).

1. Introduction

In recent years polycyclic aromatic hydrocarbons have found application as semiconducting materials, for example in light-emitting diodes, solar cells or thin-film transistors (TFTs).[1] Apart from polymeric organic semiconductors, small molecules such as acene or rylene derivatives have been widely studied in organic TFTs.[2] While numerous p-channel semiconducting materials with high hole mobilities are known, the development of air-stable n-channel semiconducting materials that possess sufficiently high electron mobilities remains a challenge. Incorporation of electron-withdrawing substituents such as halogen atoms or perfluorinated alkyl groups, leading to lower lowest unoccupied molecular orbital (LUMO) energies and increased electron affinities, are common strategies to improve material

stability and electron mobility under ambient conditions.[3] High electron affinities and low-lying LUMO energy levels facilitate the injection of electrons and lead to air-stable radical anionic species.[4]

We reported very recently on the synthesis of 2,9-bis(perfluoroalkyl)-substituted tetraazaperopyrenes (TAPPs) and their tetrachlorinated analogs[5] which displayed n–channel semiconducting behaviour. Organic thin-film transistors fabricated with these TAPPs as semiconducting material could be operated under ambient conditions and displayed excellent long-term stability.[5] This class of compounds remains otherwise entirely unexplored to date.

In order to further investigate the semiconducting properties of tetraazaperopyrenes, we now report the synthesis of the analogous core-brominated tetraazaperopyrenes, along with their crystal structures and electrochemistry. These materials also show n-channel semiconducting properties in organic field-effect transistors fabricated by vacuum deposition or by solution-based processing methods. In addition to individual TFTs with good performance and stability, we also demonstrate the fabrication of a complementary ring oscillator on a flexible substrate (PEN) using a brominated TAPP derivative for the n-channel TFTs.

2. Results and Discussion

2.1. Synthesis of the Core-Brominated 2,9-bis(Perfluoroalkyl)-Substituted Tetraazaperopyrenes (TAPPs)
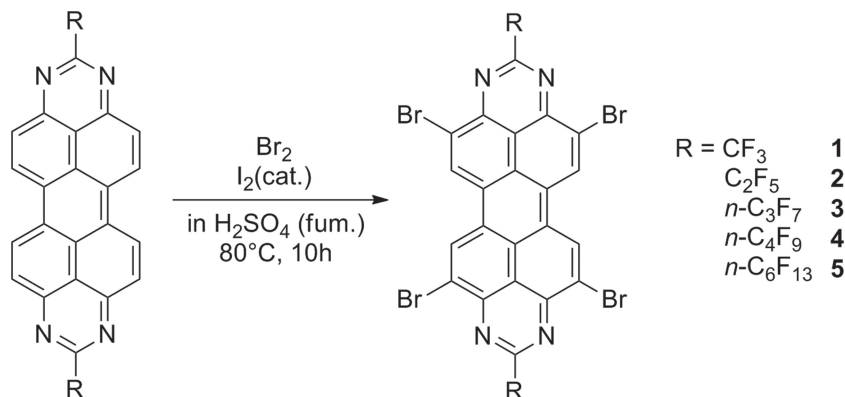
The synthetic route to core-brominated tetraazaperopyrenes is depicted in **Scheme 1**. By reacting the 2,9-bis(perfluoroalkyl)-substituted tetraazaperopyrenes[5] with a large excess of bromine in fuming sulphuric acid (20% SO$_3$) the fourfold brominated species were selectively obtained in good yields. All brominated TAPP congeners are bright orange solids that are soluble in common polar organic solvents like THF. It is remarkable that even though a large excess of bromine is used only four bromine substituents are introduced at the aromatic core. We attribute this reactivity to the different size of the orbital coefficients at the peropyrene core in strong acids such

Dr. S. Geib, Prof. H. Wadepohl, Prof. L. H. Gade
Anorganisch-Chemisches Institut
Universität Heidelberg
Im Neuenheimer Feld 270, 69120 Heidelberg, Germany
E-mail: lutz.gade@uni-hd.de
Dr. U. Zschieschang, Dr. H. Klauk
Max Planck Institute for Solid State Research
Heisenbergstr. 1, 70569 Stuttgart, Germany
E-mail: h.klauk@fkf.mpg.de
M. Gsänger, Dr. M. Stolte, Prof. F. Würthner
Institut für Organische Chemie and Center for Nanosystems Chemistry
Universität Würzburg
Am Hubland, 97074 Würzburg, Germany

DOI: 10.1002/adfm.201203600

as sulphuric acid. The theoretically modelled molecular frontier orbitals of protonated TAPP have been published earlier.[6] Since the orbital coefficients at the 4,7,11,14-positions (ortho positions) are much larger than the ones at the 5,6,12,13-positions (bay positions), an electrophilic attack is much more likely to take place in the ortho positions. All compounds were fully characterized by NMR, high resolution mass spectrometry and elemental analysis (see Experimental Section for synthetic details and full characterization data). We note that as previously observed for the core-chlorinated derivatives, core-bromination increases the solubility of the TAPPs. This is consistent with analogous observations for perylene diimide derivatives.[7]

2.2. Crystal Structures

Single crystals of compounds **2** and **3**, that were suitable for X-ray diffraction, were grown by sublimation at 370 °C in a horizontal glass tube in a weak stream of nitrogen. Both crystallise in the triclinic crystal system with the $P\overline{1}$; space group and the solid-state structures display crystallographic C_i molecular symmetry. As an example, the molecular structure of **3** is shown in **Figure 1**. The molecules are characterized by the nearly planar peropyrene core and the perfluoroalkyl-chains that point to opposite directions with respect to the aromatic plane. The bond lengths and angles of the aromatic core are nearly identical in both structures. In comparison to the known 2,9–bis(perfluoroalkyl)-TAPPs with no or chlorine substituents at the core,[5] the brominated congeners exhibit a slightly more pronounced torsion of the peropyrene core (approx. 2.2° to 2.4°, see **Table 1**). The larger van der Waals radius of the bromine atoms might lead to this torsion in order to satisfy the steric demand of the four core substituents in the solid state. The relatively small twist and the similar bond lengths and angles of the peropyrene core can be attributed to the completely conjugated, rigid aromatic system. As an example, the molecular structure of **3** is shown in Figure 1.

The packing pattern of both compounds is characterized by a slip-stacked face-to-face arrangement of the molecules (**Figure 2**) that is quite similar to the one observed for *N,N′*–bis(heptafluorobutyl)3,4:9,10-perylene diimide.[3b] Within the parallel stacks the molecules of TAPP **2** and **3** are displaced with respect to one another along the two perpendicular pseudo C_2 molecular axes along the cell axis *a* in a way which minimizes steric repulsion due to the perfluorinated side chains and bromine atoms. The perpendicular distance between the

Scheme 1. Synthetic route to fourfold core-brominated TAPP-derivatives.
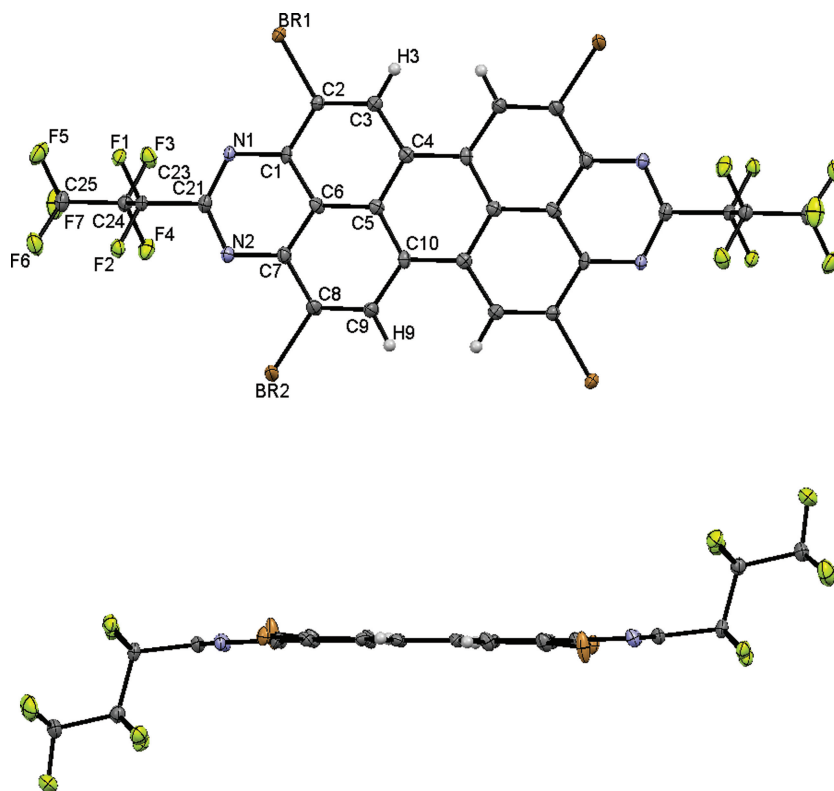
Figure 1. Top view (top) and side view (bottom) of compound **3**. Thermal ellipsoids are drawn at the 50% probability level. Selected bond lengths [Å]: C(21)-C(23) 1.527(5); N(1)-C(21) 1.327(5); N(1)-C(1) 1.353(5), N(2)-C(7) 1.342(5), C(1)-C(6) 1.416(5), C(1)-C(2) 1.442(5), C(2)-C(3) 1.355(5), C(3)-C(4) 1.437(5), C(4)-C(5) 1.434(5), C(4)-C(10)' 1.418(5), C(5)-C(6) 1.418(5), Br(1)-C(2) 1.873(3).

Table 1. Crystallographic data of compounds **2** and **3**.

	2	3
crystal system	triclinic	triclinic
space group	$P\overline{1}$;	$P\overline{1}$;
π–π-plane distance	3.38 Å	3.39 Å
packing density	2.310 g cm⁻³	2.409 g cm⁻³
torsion angle[a]	+2.2(7)°	+2.4(6)°

[a]Torsion angle between the naphthalene units C3-C4-C10′-C9′.

Figure 2. Packing pattern of tetraazaperopyrene **2** in the solid state.

Table 2. Cyclovoltammetric data and LUMO energies derived thereof, calculated LUMO energies and electron affinities.

	E_{Red1}[a] [V]	E_{Red2}[a] [V]	$E_{LUMO(CV)}$[b] [eV]	$E_{LUMO(DFT)}$[c] [eV]	EA[d] [eV]
1	−0.18	−0.56	−4.03	−4.08	3.33
2	−0.17	−0.55	−4.04	−4.09	3.37
3	−0.18	−0.56	−4.04	−4.10	3.40
4	−0.18	−0.58	−4.05	−4.11	3.42
5	−0.18	−0.56	−4.03	−4.12	3.43

[a]Measured against SCE in THF; [b]Determined according to literature methods using Fc/Fc$^+$ as an internal standard (E_{HOMO}(Fc) = −4.8 eV);[10] [c]Calculated at the B3PW91/6-31g(d,p) level of theory; [d]Calculated at the B3PW91/6-311+(g,d) level of theory.

This observation is also in good agreement with the theory that a lower number of C-H contacts in polycyclic aromatic hydrocarbons leads to more graphite-like, closely packed structures.[8] From a crystallographic point of view, the interplanar distance and the significant π-overlap should be beneficial for charge transport within an organic layer that is built up of these tetraazaperopyrene derivatives.

2.3. Cyclic Voltammetry and Theoretical Modelling

The highest occupied molecular orbital (HOMO) and LUMO energies of an organic molecule are key parameters determining whether holes or electrons will predominantly be transported in a thin-film transistor, which has been fabricated with this organic material. In the case of n-type semiconductors LUMO energies below approximately −3.7 eV are thought to be beneficial in order to obtain air-stable electric devices that can be operated under ambient conditions.[9] Furthermore, energetically low-lying LUMO levels facilitate electron injection from high-workfunction noble metal contacts like gold.[4a]

In a first step, the frontier orbital molecular energies and electron affinities were modelled by DFT using the B3PW91 functional and a 6-31g(d,p) basis set (and a 6-311+g(d,p) basis set to model the adiabatic electron affinities (EA)). The optimized structures were in good agreement with the metric parameters established from the crystal structures of **2** and **3** (see Supporting Information). The calculated HOMO and LUMO energies are summarized in **Table 2**. In order to substantiate the results from these calculations, the electrochemical properties of the tetraazaperopyrenes **1–5** were studied with cyclic voltammetry (CV). The cyclic voltammograms display two reversible reduction waves that correspond to the sequential formation of the mono- and dianion (**Figure 3**a). By using ferrocene as an internal standard, a correlation between the reduction potentials of the perylene derivatives and their LUMO energies was feasible (Table 2).[10]

Due to the fact that the carbon atoms 2 and 9 lie in a nodal plane of the frontier molecular orbitals of 2,9-bis-substituted tetraazaperopyrenes (Figure 3b),[5,11] the increasing chain length of the perfluoroalkyl substituents does not significantly influence the electrochemical properties of the derivatives **1–5**.

planes of two neighbouring molecules is 3.38 Å and 3.39 Å, respectively. It has been proposed that the self-segregation of densely packed fluorocarbon chains from the aromatic cores provides a kinetic barrier to the diffusion of ambient oxidants which has been proven advantageous for TFT applications.[3a,b] The stability under ambient conditions may result from such a structural arrangement combined with the hydrophobic effect resulting from the combination of close packing and perfluoroalkyl chains.

The substitution of hydrogen atoms by bromine leads to a decrease of the intramolecular distance between neighbouring molecules, as the distance between two C_3F_7-tetraazaperopyrene-derivatives with no core substituents was previously reported to be 3.51 Å.[5] This decrease may in part be due to the slippage of neighbouring parallel oriented molecules along both principal molecular axes, in contrast to the unidimensional displacement along the long molecular axis observed in the packing of the reference compound. The former leads to a reduction in contact area between the adjacent aromatic planes and thus reduction in possible repulsive interactions. A consequence is the observed contraction of the inter-plane distance.

Materials Views
www.MaterialsViews.com

ADVANCED
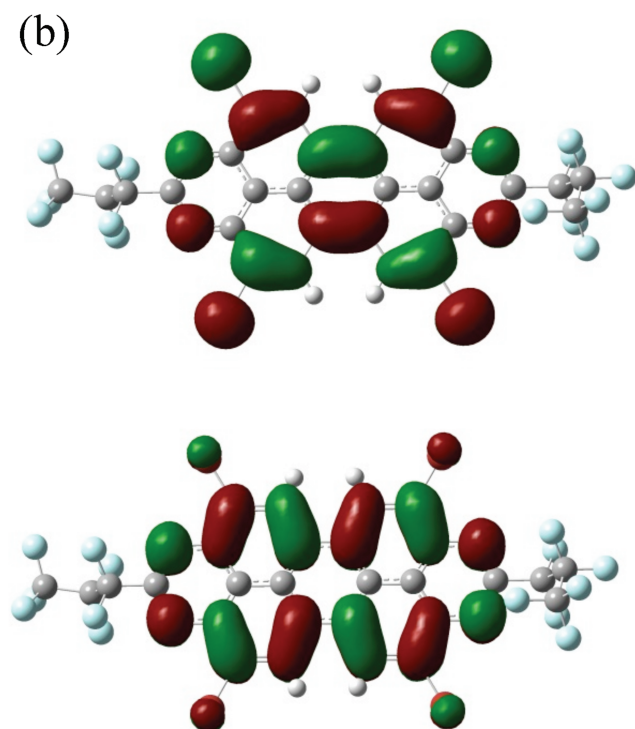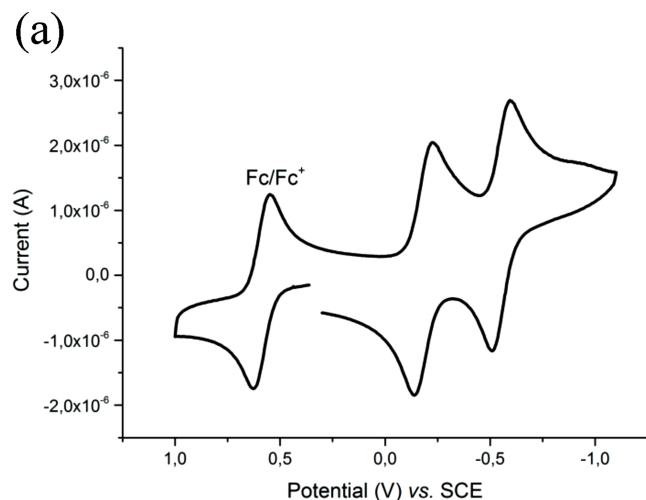FUNCTIONAL
MATERIALS
www.afm-journal.de

FULL PAPER

(a)

(b)

Figure 3. a) Cyclic voltammogramm of **1** (recorded in THF, sweep rate 50 mV/s, supporting electrolyte $^{n}Bu_4NPF_6$). b) Visualized molecular frontier orbitals, HOMO (top) and LUMO (bottom), of compound **3**.

The first and second reduction potentials are more positive than −0.66 V vs. SCE, indicating that the core-brominated TAPP derivatives should be stable against H_2O reduction.[3a,12] The LUMO energies that can be derived from the cyclovoltammetric data are smaller than −4.0 eV, and the figures that were obtained from DFT calculations are in very good agreement with these values (Table 2). This shows that the chosen computational method is well-suited for the prediction of the electronic properties of tetraazaperopyrenes. Additionally,
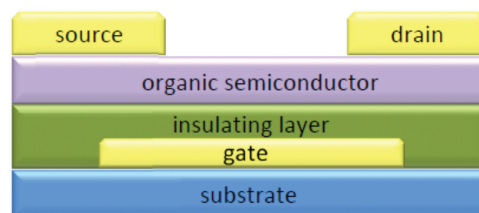
Figure 4. Schematic drawing of a bottom-gate, top-contact organic thin-film transistor composed of a gate electrode on a substrate, an insulating dielectric, the organic semiconductor thin-film as well as source and drain electrodes.

electron affinities of about 3.4 eV were calculated for the tetraazaperopyrenes **1**–**5**. The low LUMO energies as well as the high electron affinities clearly indicate that the four-fold core-brominated tetraazaperopyrenes should possess n–channel semiconducting properties.

2.4. Fabrication of Organic Transistors

Given the fact that the electrochemical data of all tetraazaperopyrene derivatives **1**–**5** render them potential n-channel semiconducting materials, their electrical properties were studied in thin-film transistors with a bottom-gate, top-contact architecture (**Figure 4**). Electron mobilities (μ_n), on/off current ratios (I_{on}/I_{off}), threshold voltages (V_{th}) and subthreshold swings (SS) were extracted from the current-voltage characteristics.[13] The electron mobilities were determined in the saturation regime.

2.4.1. TFTs Fabricated by Vacuum Deposition of the Organic Semiconductor

For TFTs operating with a thick gate dielectric a doped silicon wafer was used as substrate which also served as the gate electrode. The gate dielectric was a combination of SiO_2 (thickness: 100 nm), AlO_x (thickness: 8 nm) and a tetradecylphosphonic acid self-assembled monolayer (SAM, thickness: 1.7 nm). For TFTs with thin gate dielectric, Al (thickness: 20 nm) was deposited onto a doped silicon substrate. The gate dielectric was a combination of AlO_x (thickness: 3.6 nm) and a tetradecylphosphonic acid SAM (thickness: 1.7 nm).

All TFTs exclusively display n-channel semiconducting properties. They operated in air without encapsulation and showed excellent stability under ambient conditions. The electrical parameters measured on TFTs with a vacuum-deposited semiconducting layer are summarized in **Table 3**. The optimum substrate temperature was individually determined for each compound.

The best performance of $\mu_n = 0.032$ cm^2/V s was measured for compound **3**, which contains two heptafluoropropyl substituents at the 2 and 9 position. The observation that heptafluoropropyl substituents provide optimum TFT performance has also been made previously in our group for the unsubstituted and the core-chlorinated tetraazaperopyrenes[5] as well as for 2,6-dichloro-substituted naphthalene diimides.[14] The current-voltage characteristics of TFTs with compound **3** deposited in vacuum having either a thick or a thin gate dielectric are

Table 3. Summary of the electrical parameters measured in air of TFTs that were fabricated by vacuum deposition of the tetraazaperopyrenes **1**–**5**.

	T_{sub} [°C]	TFTs with thick SiO$_2$/AlO$_x$/SAM gate dielectric				TFTs with thin AlO$_x$/SAM gate dielectric			
		μ_n [cm^2/Vs]	I_{on}/I_{off}	V_{th} [V]	SS [V decade^{-1}]	μ_n [cm^2/Vs]	I_{on}/I_{off}	V_{th} [V]	SS [V decade^{-1}]
1	80	0.0004	5×10^3	17	5.3	0.000016	5×10^2	0.6	1.1
2	90	0.028	10^5	13	2.2	0.004	10^4	0.8	0.2
3	70	0.032	5×10^5	18	1.8	0.032	5×10^4	0.9	0.24
4	90	0.007	3×10^5	11	2.2	0.003	5×10^3	0.8	0.32
5	100	0.003	5×10^3	18	3.5	no field-effect			

depicted in **Figure 5**. The thin gate dielectric has the advantage that the transistors can be operated with lower voltages.

As compound **3** is the derivative that exhibits the largest electron mobilities in TFTs, its long-term air stability was monitored. After storing TFTs in ambient air (relative humidity ≈40%) for 200 days, an electron mobility of 0.02 cm^2/V s was measured, i.e., the electron mobility of TFTs based on compound **3** is relatively stable during prolonged air exposure.

2.4.2. Organic Transistors Based on Solution-Deposited Semiconductors

Since the core-brominated tetraazaperopyrenes displayed good solubility in polar organic solvents we investigated their behaviour and performance in organic thin-film transistors with semiconducting layers that were processed from the liquid phase. In first attempts, spin coating and drop casting experiments were carried out with the brominated TAPPs in THF (concentration 5 mg/mL). For TFTs that were fabricated via spin coating on a 100 nm SiO$_2$ dielectric, only small electron mobilities of approx. 10^{-8} cm^2/V s were measured for

compound **2** and **4**. TFTs that were fabricated via drop casting showed charge carrier mobilities of approx. 10^{-5} cm^2/V s for compound **3** and **4**. These low values might be attributed to the low level of crystallinity and order of the organic layer that is generated by these two methods.[15] Consequently, as a third method, solution shearing[16] was applied to deposit the organic semiconductor layer onto the Si substrate. Solution shearing is a suitable method for generating highly crystalline and ordered thin-films on planar substrates. Organic semiconductor layers that have been fabricated by shearing are characterized by larger crystal domains that are aligned along the shearing direction. Such a morphology has been reported to be beneficial for TFT performance and devices that have been processed via shearing exhibit higher charge-carrier mobilities than devices that have been fabricated via other solution-based methods.[16]

Since tetraazaperopyrene **3** displayed the highest electron mobilities in thin-film transistors fabricated via vacuum deposition of the organic semiconductor, solution shearing experiments were exclusively carried out with compound **3**. A highly doped n-type Si (100) wafer with a 100 nm SiO$_2$ layer, that served as gate dielectric, was used as the substrate. The
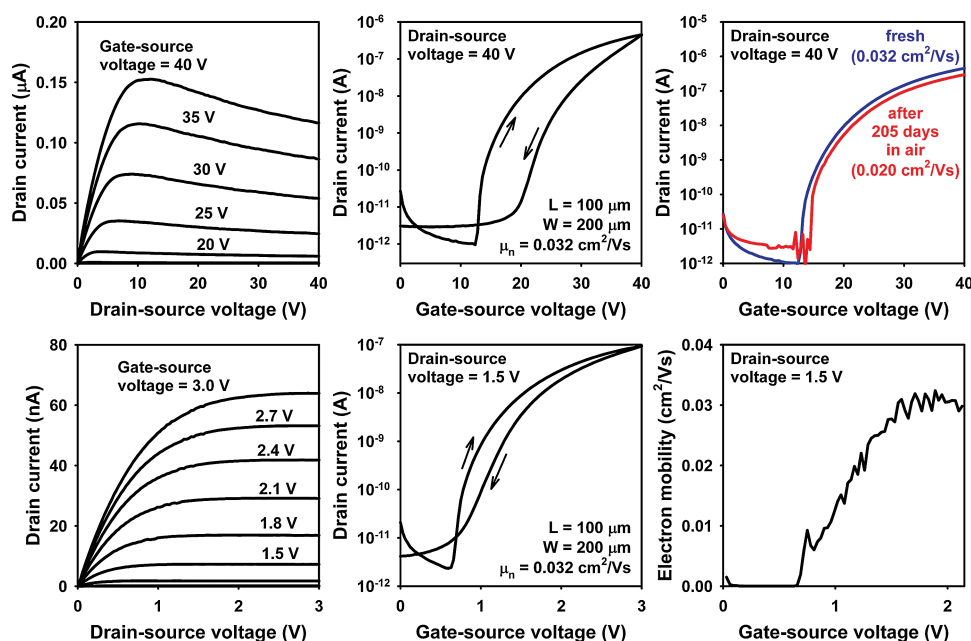

Figure 5. Current-voltage characteristics of TFTs with a vacuum-deposited layer of **3** as the semiconductor fabricated on silicon substrates. Top: thick gate dielectric (100 nm SiO$_2$ + 8 nm AlO$_x$ + SAM). Bottom: thin gate dielectric (3.6 nm AlO$_x$ + 1.7 nm SAM).

Table 4. Summary of the mean electrical properties of OTFTs of solution-sheared TAPP **3** with regard to the shearing direction per six devices each.

	parallel to shearing direction	perpendicular to shearing direction
μ [cm^2/Vs]	0.011 ± 0.002	0.0006 ± 0.0004
I_{on}/I_{off}	3.0×10^4	2.0×10^3
V_{th} [V]	1.6 ± 0.2	1.8 ± 0.5

shearing tool was obtained by treating a silicon wafer with octa-decyltriethoxysilane (OTES) as described in the literature to be highly de-wetting.[17] For solution shearing, a solution of 2 mg/mL of compound **3** in *ortho*-dichlorobenzene was prepared and pre-heated to 100 °C. The Si wafer and the shearing tool were pre-heated to 130 °C prior to use and a shearing velocity of 0.08 mm/s was employed. The thin-film deposition as well as all measurements of the electrical properties were carried out in air.

A shearing angle of 0° did not lead to a closed crystalline layer, but for shearing angles of 15° and 30° closed layers with optical anisotropy could be observed under a cross-polarized light microscope (see Supporting Information). However, the highest electron mobilities were measured for thin-films deposited with 15° angle and a strong anisotropy in effective charge carrier mobility with respect to the shearing direction was observed. Transistors that were measured parallel to the shearing direction showed electron mobilities of up to 0.013 cm^2/V s whereas transistors that were measured perpendicular to the shearing direction only showed values of 0.0006 cm^2/V s. The mean TFT parameters measured parallel and perpendicular to the shearing direction are summarized in **Table 4**. **Figure 6** shows the output and transfer characteristics of a TFT that was fabricated by solution shearing of compound **3** in parallel orientation with regard of the shearing direction.

Comparison of the data listed in Table 3 and 4 reveals that the effective electron mobility and the on/off ratio of the solution-deposited TFTs, with the current flowing parallel to the shearing direction, are only slightly smaller (0.013 cm^2/V s, 3×10^4) than those of the TFTs with the vacuum-deposited semiconductor (0.032 cm^2/Vs , 5×10^5). It is also interesting to note that the threshold voltage of the solution-processed TFTs is much closer to zero (1–2 V) than that of the vacuum-deposited TFTs (18 V). It is difficult to say, however, whether this difference in threshold voltage is related to the different semiconductor deposition methods (solution shearing vs.

vacuum deposition) or to the different gate dielectrics (SiO$_2$ without SAM modification for the solution-sheared TFTs vs. SiO$_2$+AlO$_x$+SAM for the vacuum-deposited TFTs). Solution shearing is therefore a versatile method to rapidly produce large-area thin-films of TAPP **3** from solution with appreciable electron mobility in air.

2.5. Complementary Inverters and Ring Oscillators

We fabricated complementary inverters as well as 5-stage complementary ring oscillators on flexible plastic substrates, using compound **3** as the semiconductor for the n-channel TFTs and dinaphtho-[2,3-b:2′,3′–f]thieno[3,2–b]thiophene (DNTT)[18] as the semiconductor for the p-channel TFTs. The fabrication process for the complementary inverters and ring oscillators is identical to that described previously,[5] except for the substrate which is PEN rather than glass.

Polyethylene naphthalate (PEN, thickness: 125 μm) was used as the substrate. Al (thickness: 20 nm) was deposited by thermal evaporation through a shadow mask to define the patterned gate electrodes. The gate dielectric was a combination of AlO$_x$ (thickness: 3.6 nm) and a tetradecylphosphonic acid SAM (thickness: 1.7 nm). The tetraazaperopyrene derivative **3** (for the n-channel TFTs) and DNTT (for the p-channel TFTs) were vacuum-deposited onto the gate dielectric to form organic semiconductor layers with a thickness of 25 to 30 nm. As the last step, the Au source and drain contacts were deposited on top of the semiconducting layer by thermal evaporation in vacuum through a shadow mask. All electrical measurements were carried out in air.

The static transfer characteristics of an inverter are shown in **Figure 7** and a representative output signal of a ring oscillator is shown in **Figure 8**, along with the signal propagation delay per stage as a function of supply voltage measured on ring oscillators based on TFTs with channel lengths of 20 and 30 μm. Also shown in Figure 8 is a comparison with literature data of the stage delay of flexible organic complementary ring oscillators.[19] For supply voltages between 0.5 and 4 V, our ring oscillators based on tetraazaperopyrene derivative **3** and a channel length of 20 μm provide the shortest stage delay reported thus far for such ring oscillators. For supply voltages between 5 and 20 V, the best dynamic performance for flexible organic complementary ring oscillators is that reported by Smaal et al., who used Polyera ActivInk N3300 as the n-channel semiconductor and implemented TFTs with a channel length of 5 μm.[19h]

3. Conclusion

In summary we have presented a straightforward synthesis that selectively leads to fourfold core-brominated tetraazaperopyrene derivatives. Since these novel core-brominated TAPPs possess low LUMO energy levels and high electron affinities, their semiconducting properties were studied in organic thin-film transistors that were fabricated both by
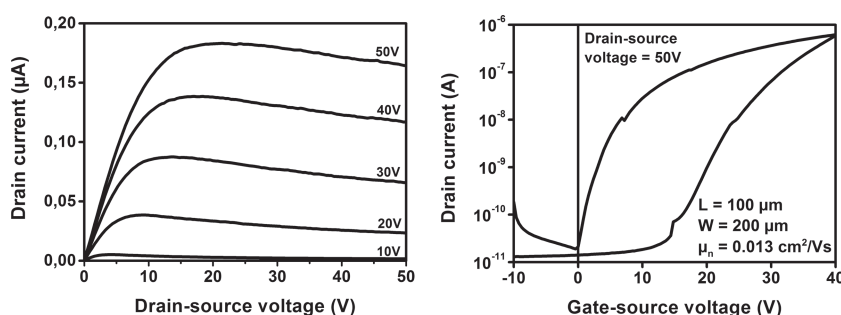
Figure 6. Output and transfer characteristics of a TFT of TAPP **3** in parallel orientation with regard to the shearing direction.

FULL PAPER
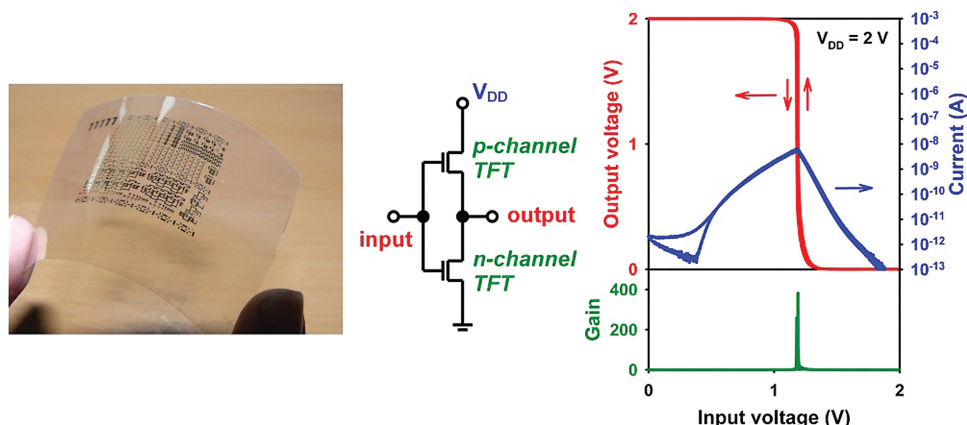
Figure 7. Static characteristics of flexible organic complementary inverters based on compound **3** as the n-channel semiconductor. Left: photograph of the substrate. Center: circuit schematic of a complementary inverter. Right: inverter transfer characteristics.
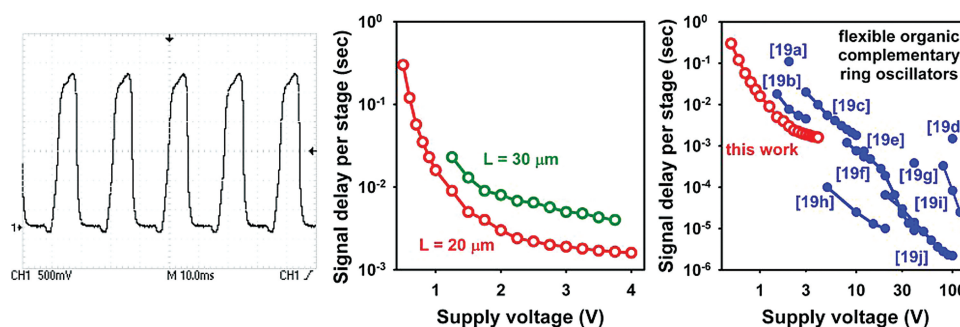
Figure 8. Dynamic performance of flexible organic complementary ring oscillators based on compound **3** as the n-channel semiconductor. Left: output signal (channel length: 20 μm, supply voltage: 3 V). Center: stage delay as a function of supply voltage. Right: literature comparison.[19]

vacuum deposition of the organic layer as well as solution processing. All five compounds exhibit n-channel semiconducting properties and the highest electron mobility of 0.032 cm²/V s was found for compound **3**. With compound **3**, 5-stage complementary ring oscillators were fabricated on flexible plastic (PEN) substrates. In addition to vacuum deposition, solution shearing of compound **3** was employed as a faster and simpler processing method. The highest electron mobility was measured parallel to the shearing direction with μ_n = 0.013 cm²/V s. The brominated TAPP derivatives have displayed remarkable stability under ambient conditions over periods of over 6 months. In particular, they offer an entry into the systematic development of derivatives generated by catalytic C-C and C-X- coupling to be developed in future studies.

Bromine substitution has been studied for other families of organic semiconductors. Jones et al.[20a] reported that the field-effect mobilities of n-channel TFTs based on dioctyl-dibromo-perylene tetracarboxylic diimide (PTCDI-Br$_2$-(C$_8$H$_{17}$)$_2$) are much smaller than those obtained with the unsubstituted parent compound (PTCDI-(C$_8$H$_{17}$)$_2$) or the dicyano-substituted derivative (PTCDI-(CN)$_2$-(C$_8$H$_{17}$)$_2$). This might suggest that bromine substitution is detrimental, but there are too many differences between the molecules studied by Jones et al.[20a] and those studied here to allow a meaningful comparison (dioctyl-PTCDI vs. bis(perfluorobutyl)-TAPP, ortho vs. bay position, dibromo vs. tetrabromo substitution). Schmidt et al.[3b] reported

that bis(heptafluorobutyl)-tetrabromo-perylene tetracarboxylic diimide (PTCDI-Br$_2$-(CH$_2$C$_3$F$_7$)$_2$) gives smaller electron mobilities than compounds with tetrafluoro or tetrachloro substitution or without core substitution. Again, there is an important difference (ortho vs. bay position) that prevents a meaningful comparison. Finally, Usta et al.[20b] compared dioctyl- and bis(heptafluorobutyl)-anthracene-dicarboximide derivatives with dibromo and dicyano substitution and without substitution and found the best performance for dicyano substitution. Finally we would like to note that the electron mobilities reported in previous studies on bromo-substituted semiconductors[3b,20a,20b] are smaller than the electron mobility which we have measured for the TAPP derivative **3** (0.032 cm²/V s).

4. Experimental Section

Materials and Methods: The 2,9-bis(perfluoroalkyl)-1,3,8,10-tetraazaperopyrenes were synthesized as reported previously.[5] Bromine and fuming sulphuric acid (20% SO$_3$) were purchased from Aldrich and used as received. ¹H and ¹³C NMR spectra were recorded on a Bruker Avance III spectrometer and ¹⁹F NMR spectra on a Bruker Avance II spectrometer at 295K. FAB mass spectra were obtained from a JEOL JMS-700 and MALDI mass spectra from a Bruker apex-Qe FT-ICR spectrometer. Elemental analyses were carried out in the Microanalytical Laboratory at the Chemistry Department at the University of Heidelberg on a vario MICRO cube from Elementar.

Synthesis: *General Procedure for the Preparation of Fourfold Core-Brominated TAPP-Derivatives*: 2.00 mmol of the corresponding 2,9-bis(perfluoroalkyl)-1,3,8,10-tetraazaperopyrene were dissolved in 75 mL fuming sulphuric acid. 100 mg (0.40 mmol) iodine and 3 mL (60.00 mmol) bromine were added. The reaction mixture was heated to 80 °C for 10 h, cooled to room temperature and poured on ice. The resulting precipitate was collected by filtration and washed thoroughly with aqueous sodium hydroxide, water, methanol and pentane and dried in vacuo. The obtained solid was sublimed in vacuo for further purification to give a bright orange solid.

2,9-Bis(trifluoromethyl)-4,7,11,14-tetrabromo-1,3,8,10-tetraazaperopyrene (1): Synthesized according to the general bromination procedure described above. Starting material: 935 mg 2,9-bis(trifluoromethyl)-1,3,8,10-tetraazaperopyrene. Yield: 803 mg (1.02 mmol, 51%). ^{1}H NMR (600.13 MHz, d$_8$-THF, δ): 10.67 (s, 4H, C^{3}H). ^{13}C NMR (150.92 MHz, d$_8$-THF, δ): 157.8 (q, $^2J_{CF}$ = 41.0 Hz, C^{21}), 152.4 (C^1), 136.2 (C^3), 127.4 (C^2), 125.9 (C^4), 119.9 (C^5), 118.0 (C^6), 115.1 (q, $^1J_{CF}$ = 286.0 Hz, CF$_3$). ^{19}F NMR (376.27 MHz, d$_8$-THF, δ): −68.76 (s, 6F, CF$_3$). HR-MS (FAB$^+$, m/z) calcd. for C$_{24}$H$_5$^{79}Br$_2$^{81}Br$_2$F$_6$N$_4$: 782.7111; found: 782.7130. Anal. calcd. for C$_{24}$H$_4$Br$_4$F$_6$N$_4$: C 36.87 H 0.52 N 7.17; found: C 37.06 H 0.76 N 7.29.

2,9-Bis(pentafluoroethyl)-4,7,11,14-tetrabromo-1,3,8,10-tetraazaperopyrene (2): Synthesized according to the general bromination procedure described above. Starting material: 1.13 g 2,9-bis(pentafluoroethyl)-1,3,8,10-tetraazaperopyrene. Yield: 1.32 g (1.50 mmol, 75%). ^{1}H NMR (600.13 MHz, d$_8$-THF, δ): 10.68 (s, 4H, C^{3}H). ^{13}C NMR (150.92 MHz, d$_8$-THF, δ): 155.6 (C^{21}), 152.3 (C^1), 136.2 (C^3), 127.5 (C^2), 125.9 (C^4), 119.9 (C^5), 117.7 (C^6). Perfluorinated alkyl carbon signals were not resolved from underground noise. ^{19}F NMR (376.27 MHz, d$_8$-THF, δ): −82.32 (m, 6F, CF$_3$), −115.24 (m, 4F, CF$_2$). HR-MS (FAB$^+$, m/z) calcd. for C$_{26}$H$_5$^{79}Br$_2$^{81}Br$_2$F$_{10}$N$_4$: 882.7047; found: 882.7031. Anal, calcd. for C$_{26}$H$_4$Br$_4$F$_{10}$N$_4$: C 35.41 H 0.46 N 6.35; found: C 35.18 H 0.68 N 6.30.

2,9-Bis(heptafluoropropyl)-4,7,11,14-tetrabromo-1,3,8,10-tetraazaperopyrene (3): Synthesized according to the general bromination procedure described above. Starting material: 1.31 g 2,9-bis(heptafluoropropyl)-1,3,8,10-tetraazaperopyrene. Yield: 1.59 g (1.62 mmol, 81%). ^{1}H NMR (600.13 MHz, d$_8$-THF, δ): 10.68 (s, 4H, C^{3}H). ^{13}C NMR (150.92 MHz, d$_8$-THF, δ): 152.3 (C^1), 136.2 (C^3), 127.5 (C^2), 126.0 (C^4), 119.9 (C^5), 117.7 (C^6). Perfluorinated alkyl carbon signals and C^{21} were not resolved from underground noise. ^{19}F NMR (376.27 MHz, d$_8$-THF, δ): −80.93 (t, 6F, $^3J_{FF}$ = 9.1 Hz, CF$_3$), −113.60 (m, 4F, CF$_2$), −125.98 (m, 4F, CF$_2$). HR-MS (FAB$^+$, m/z) calcd. for C$_{28}$H$_5$^{79}Br$_2$^{81}Br$_2$F$_{14}$N$_4$: 982.6983; found: 982.6973. Anal. calcd. for C$_{28}$H$_4$Br$_4$F$_{14}$N$_4$: C 34.25 H 0.41 N 5.71; found: C 34.37 H 0.62 N 5.69.

2,9-Bis(nonafluorobutyl)-4,7,11,14-tetrabromo-1,3,8,10-tetraazaperopyrene (4): Synthesized according to the general bromination procedure described above. Starting material: 1.53 g 2,9-bis(nonafluorobutyl)-1,3,8,10-tetraazaperopyrene. Yield: 1.48 g (1.36 mmol, 69%). ^{1}H NMR (600.13 MHz, d$_8$-THF, δ): 10.65 (s, 4H, C^{3}H). ^{13}C NMR (150.92 MHz, d$_8$-THF, δ): 153.6 (C^1), 137.6 (C^3), 128.8 (C^2), 127.2 (C^4), 121.2 (C^5), 119.0 (C^6). Perfluorinated alkyl carbon signals and C^{21} were not resolved from underground noise. ^{19}F NMR (376.27 MHz, d$_8$-THF, δ): −81.77 (t, 6F, $^3J_{FF}$ = 10.0 Hz, CF$_3$), −112.79 (m, 4F, CF$_2$), −122.19 (m, 4F, CF$_2$), −125.87 (m, 4F, CF$_2$). HR-MS (MALDI$^+$, m/z) calcd. for C$_{30}$H$_5$^{81}Br$_4$F$_{18}$N$_4$: 1086.6872; found: 1086.6842. Anal. calcd. for C$_{30}$H$_4$Br$_4$F$_{18}$N$_4$: C 33.30 H 0.37 N 5.18; found: C 33.72 H 0.60 N 5.32.

2,9-Bis(tridecafluorohexyl)-4,7,11,14-tetrabromo-1,3,8,10-tetraazaperopyrene (5): Synthesized according to the general bromination procedure described above. Instead of filtration, the product was isolated by extraction with ethyl acetate from the aqueous phase. Starting material: 1.93 g 2,9-bis(tridecafluorohexyl)-1,3,8,10-tetraazaperopyrene. Yield: 744 mg (0.58 mmol, 29%). ^{1}H NMR (600.13 MHz, d$_8$-THF, δ): 10.67 (s, 4H, C^{3}H). ^{13}C NMR (150.92 MHz, d$_8$-THF, δ): 155.8 (t, $^2J_{CF}$ = 25.6 Hz, C^{21}), 153.5 (C^1), 137.5 (C^3), 128.8 (C^2), 127.2 (C^4), 121.2 (C^5), 118.9 (C^6). Perfluorinated alkyl carbon signals were not resolved from underground noise. ^{19}F NMR (376.27 MHz, d$_8$-THF, δ): −81.73 (t, 6F, $^3J_{FF}$ = 10.1 Hz, CF$_3$), −112.61 (m, 4F, CF$_2$), −121.24 (m, 4F, CF$_2$), −121.56 (m, 4F, CF$_2$), −123.15 (m, 4F, CF$_2$), −126.72 (m, 4F, CF$_2$). HR-MS (MALDI$^+$, m/z)

calcd. for C$_{34}$H$_5$^{79}Br^{81}Br$_3$F$_{26}$N$_4$: 1284.6766; found: 1284.6750. Anal. calcd. for C$_{34}$H$_4$Br$_4$F$_{26}$N$_4$: C 31.85 H 0.31 N 4.37; found: C 32.13 H 0.51 N 4.47.

Crystallographic data (excluding structure factors) for the structure(s) reported in this paper have been deposited with the Cambridge Crystallographic Data Centre as supplementary publication no. CCDC-911239 and 911240.

Supporting Information

Supporting Information is available from the Wiley Online Library or from the author.

Acknowledgements

[1] a) S. R. Forrest, M. E. Thompson, *Chem. Rev.* **2007**, *107*, 923; b) J. Baffreau, S. Leroy-Lhez, H. Derbal, A. R. Inigo, J.-M. Nunzi, M. M. Groeneveld, R. M. Williams, P. Hudhomme, *Eur. Phys. J. Appl. Phys.* **2007**, *36*, 301; c) S. Günes, H. Neugebauer, N. S. Sariciftci, *Chem. Rev.* **2007**, *107*, 1324; d) T. M. Figueira-Duarte, K. Müllen, *Chem. Rev.* **2011**, *111*, 7260; e) A. C. Grimsdale, K. L. Chan, R. E. Martin, P. G. Jokisz, A. B. Holmes, *Chem. Rev.* **2009**, *109*, 897; f) J. Zaumseil, H. Sirringhaus, *Chem. Rev.* **2007**, *107*, 1296; g) Y. Sun, Y. Liu, D. Zhu, *J. Mater. Chem.* **2005**, *15*, 53; h) C. Di, Y. Liu, G. Yu, D. Zhu, *Acc. Chem. Res.* **2009**, *42*, 1573.

[2] a) W. Wu, Y. Liu, D. Zhu, *Chem. Soc. Rev.* **2010**, *39*, 1489; b) C. Wang, H. Dong, W. Hu, Y. Liu, D. Zhu, *Chem. Rev.* **2012**, *112*, 2208; c) F. Würthner, M. Stolte, *Chem. Commun.* **2011**, *47*, 5109.

[3] a) B. A. Jones, A. Facchetti, M. R. Wasielewski, T. J. Marks, *J. Am. Chem. Soc.* **2007**, *129*, 15259; b) R. Schmidt, J. H. Oh, Y.-S. Sun, M. Deppisch, A.-M. Krause, K. Radacki, H. Braunschweig, M. Könemann, P. Erk, Z. Bao, F. Würthner, *J. Am. Chem. Soc.* **2009**, *131*, 6215; c) A. Lv, S. R. Puniredd, J. Zhang, Z. Li, H. Zhu, W. Jiang, H. Dong, Y. He, L. Jiang, Y. Li, W. Pisula, Q. Meng, W. Hu, Z. Wang, *Adv. Mater.* **2012**, *24*, 2626; d) H. Qian, F. Negri, C. Wang, Z. Wang, *J. Am. Chem. Soc.* **2008**, *130*, 17970; e) H. Usta, A. Facchetti, T. J. Marks, *Acc. Chem. Res.* **2011**, *44*, 501.

[4] a) H. Klauk, *Chem. Soc. Rev.* **2010**, *39*, 2643; b) Y.-C. Chang, M.-Y. Kuo, C.-P. Chen, H.-F. Lu, I. Chao, *J. Phys. Chem. C* **2010**, *114*, 11595.

[5] S. C. Martens, U. Zschieschang, H. Wadepohl, H. Klauk, L. H. Gade, *Chem. Eur. J.* **2012**, *18*, 3498.

[6] T. Riehm, G. De Paoli, A.E. Konradsson, L. De Cola, H. Wadepohl, L.H. Gade, *Chem. Eur. J.* **2007**, *13*, 7317.

[7] a) G. Seybold, G. Wagenblast, *Dyes Pigm.* **1989**, *11*, 303; b) G. Seybold, A. Stange, *German Patent*, DE 3545004, **1987**.

[8] M. Winkler, K. N. Houk, *J. Am. Chem. Soc.* **2007**, *129*, 1805.

[9] X. Zhan, A. Facchetti, S. Barlow, T. J. Marks, M. A. Ratner, M. R. Wasielewski, S. R. Marder, *Adv. Mater.* **2011**, *23*, 268.

[10] I. Seguy, P. Jolinat, P. Destruel, R. Mamy, H. Allouchi, C. Courseille, M. Cotrait, H. Bock, *ChemPhysChem* **2001**, *2*, 448.

[11] S. C. Martens, T. Riehm, S. Geib, H. Wadepohl, L. H. Gade, *J. Org. Chem.* **2011**, *76*, 609.

[12] a) D. M. de Leeuw, M. M. J. Simenon, A. R. Brown, R. E. F. Einerhand, *Synth. Meth.* **1997**, *87*, 53; b) F. Würthner, *Angew. Chem.* **2001**, *113*, 1069; *Angew. Chem. Int. Ed.* **2001**, *40*, 1037.

[13] S. M. Sze, K. K. Ng, *Physics of Semiconductor Devices, 3rd ed.*, Wiley, New York **2007**.

[14] M. Stolte, S.-L. Suraru, F. Würthner, J. H. Oh, Z. Bao, J. Brill, M. Könemann, J Qu, U. Zschieschang, H. Klauk, *Proc. SPIE* **2010**, *7778*, 777804-1.

[15] J. Locklin, K. Shinbo, K. Onishi, F. Kaneko, Z. Bao, R. C. Avincula, *Chem. Mater.* **2003**, *15*, 1404.

[16] a) H. A. Becerril, M. E. Roberts, Z. H. Liu, J. Locklin, Z. Bao, *Adv. Mater.* **2008**, *20*, 2588; b) G. Giri, E. Verploegen, S. C.B. Mannsfeld, S. Atahan-Evrenk, D. H. Kim, S. Y. Lee, H. A. Becerril, A. Aspuru-Guzik, M.F. Toney, Z. Bao, *Nature* **2011**, *480*, 504; c) W.-Y. Lee, J. H. Oh, S.-L. Suraru, W.-C. Chen, F. Würthner, Z. Bao, *Adv. Funct. Mater.* **2011**, *21*, 4173; d) M. Stolte, M. Gsänger, R. Hofmockel, S.-L. Suraru, F. Würthner*Phys. Chem. Chem. Phys.* **2012**, *14*, 14181.

[17] Y. Ito, A. A. Virkar, S. Mannsfeld, J. H. Oh, M. Toney, J. Locklin, Z. Bao, *J. Am. Chem. Soc.* **2009**, *131*, 9396.

[18] U. Zschieschang, F. Ante, D. Kälblein, T. Yamamoto, K. Takimiya, H. Kuwabara, M. Ikeda, T. Sekitani, T. Someya, J. Blochwitz-Nimoth, H. Klauk, *Org. Electron.* **2011**, *12*, 1370.

[19] a) K. Ishida, N. Masunaga, R. Takahashi, T. Sekitani, S. Shino, U. Zschieschang, H. Klauk, M. Takamiya, T. Someya, T. Sakurai, *IEEE J. Solid-State Circuits* **2011**, *46*, 285; b) T. Sekitani, U. Zschieschang, H. Klauk, T. Someya, *Nat. Mater.* **2010**, *9*, 1015; c) J. H. Na, M. Kitamura, Y. Arakawa, *Thin Solid Films* **2009**, *517*, 2079; d) H. Kempa, M. Hambsch, K. Reuter, M. Stanel, G. C. Schmidt, B. Meier, A. C. Hübler, *IEEE Trans. Electron. Devices* **2011**, *58*, 2765; e) H. Yan, Y. Zheng, R. Blache, C. Newman, S. Lu, J. Woerle, A. Facchetti, *Adv. Mater.* **2008**, *20*, 3393; f) H. Klauk, M. Halik, U. Zschieschang, F. Eder, D. Rohde, G. Schmid, C. Dehm, *IEEE Trans. Electron Devices* **2005**, *52*, 618; g) M. Guerin, A. Daami, S. Jacob, E. Bergeret, E. Benevent, P. Pannier, R. Coppard, *IEEE Trans. Electron Devices* **2011**, *58*, 3587; h) W. Smaal, C. Kjellander, Y. Jeong, A. Tripathi, B. van der Putten, A. Facchetti, H. Yan, J. Quinn, J. Anthony, K. Myny, W. Dehaene, G. Gelinck, *Org. Electron.* **2012**, *13*, 1686; i) K. J. Baeg, J. Kim, D. Khim, M. Caironi, D. Y. Kim, I. K. You, J. R. Quinn, A. Facchetti, Y. Y. Noh, *ACS Appl. Mater. Interfaces* **2011**, *3*, 3205; j) K. J. Baeg, D. Khim, D. Y. Kim, S. W. Jung, J. B. Koo, I. K. You, H. Yan, A. Facchetti, Y. Y. Noh, *J. Polym. Sci., Part B: Polym. Phys.* **2011**, *49*, 62.

[20] a) B. A. Jones, A. Facchetti, M. R. Wasielewski, T. J. Marks, *Adv. Funct. Mater.* **2008**, *18*, 1329; b) H. Usta, C. Kim, Z. Wang, S. Lu, H. Huang, A. Facchetti, T. J. Marks, *J. Mater. Chem.* **2012**, *22*, 4459.

Supporting Information

for

Core-Brominated Tetraazaperopyrenes as n-Channel Semiconductors for Organic Complementary Circuits on Flexible Substrates

By *Sonja Geib*[a], *Ute Zschieschang*[b], *Marcel Gsänger*[c], *Matthias Stolte*[c], *Frank Würthner*[c], *Hubert Wadepohl*[a], *Hagen Klauk*[b],* and *Lutz H. Gade*[a],*

[*,a]   Prof. Dr. L. H. Gade, S. Geib, Prof. Dr. H. Wadepohl
Anorganisch-Chemisches Institut, Universität Heidelberg
Im Neuenheimer Feld 270, 69120 Heidelberg (Germany)
E-mail: lutz.gade@uni-hd.de
[*,b]   Dr. H. Klauk, Dr. U. Zschieschang
Max Planck Institute for Solid State Research
Heisenbergstr. 1, 70569 Stuttgart (Germany)
E-mail: h.klauk@fkf.mpg.de
[c]   Prof. Dr. F. Würthner, M. Gsänger, Dr. M. Stolte
Institut für Organische Chemie and Center for Nanosystems Chemistry, Universität Würzburg
Am Hubland, 97074 Würzburg (Germany)

Table of Contents

Cyclic voltammetry was performed with a standard commercial electrochemical analyser in a

three electrode single-component cell under argon. A platinum disk was used as the working

electrode, a platinum wire as the counter electrode and a saturated calomel electrode as the

reference electrode. All potentials were internally referenced to ferrocene. Dry THF was used

as solvent and the supporting electrolyte was tetrabutylammonium hexafluorophosphate. The

measurements were carried out under exclusion of air and moisture.

S2. Computational Methods

The DFT-B3PW91 functional has been employed to model the systems in this work with a 6–

31g(d,p) basis set for all atoms.[S1] The calculations have been carried out with the

GAUSSIAN03 and GAUSSIAN09 programme packages.[S2] Every optimisation was followed

by a frequency analysis to verify the energy minima. Electron affinities were determined with

a 6-311+g(d,p) basis set by optimising the structure of the neutral and the anionic species and

taking the difference of the total energies of both species.[S3]

S2.1. Cartesian coordinates of the optimized structures

with B3PW91/6-31g(d,p)

Compound **1**
```
Charge =  0 Multiplicity = 1
 C                    -5.3483    -0.02216    0.58369
 C                    -3.45541    1.2047      0.38385
 C                    -2.69915    0.00981     0.2855
 C                    -3.4293    -1.20353     0.35024
 C                    -2.75399    2.46         0.32079
 C                    -1.28834    0.02741      0.12577
 C                    -0.6173     1.28025      0.06539
 C                    -1.40007    2.47544      0.16956
 C                     0.79348    1.29778     -0.09855
 C                     1.49093    0.06222     -0.20019
 C                     0.82042   -1.19065     -0.13601
 C                    -0.59037   -1.20821      0.02896
 C                    -1.34702   -2.42248      0.09881
 C                    -2.70079   -2.44097      0.25126
 H                    -0.83753   -3.37458      0.02817
 H                    -0.9114     3.44008      0.12667
 C                     2.90006    0.08012     -0.37342
 C                     3.65477   -1.11439     -0.48371
 C                     3.6295     1.29358     -0.44637
```

```
N                           4.98228   -1.08803   -0.65722
N                           4.95678    1.3008     -0.6212
N                          -4.76022   -1.21023    0.4986
N                          -4.78657    1.17953    0.52849
C                           5.54325    0.11332   -0.72242
C                           2.95534   -2.36989   -0.40767
C                           1.60297   -2.38569   -0.2426
H                           1.1153    -3.35047   -0.1924
C                           1.55032    2.51206   -0.16767
H                           1.04191    3.46404   -0.08821
C                           2.90266    2.53079   -0.33183
C                           7.05481    0.14079   -0.95214
C                          -6.86989   -0.0492     0.74025
F                           7.46056   -1.02182   -1.50256
F                           7.35094    1.148      -1.80515
F                          -7.22979   -1.09093    1.51978
F                          -7.29402    1.09411    1.32027
Br                         -3.63864   -4.10255    0.33896
Br                          3.92912   -4.00703   -0.54776
Br                          3.84036    4.19246   -0.41931
Br                         -3.72809    4.09743    0.45523
F                          -7.4962    -0.17707   -0.44881
F                           7.80309    0.35785    0.15034
```

Compound 2

```
Charge =  0 Multiplicity = 1
C                          -5.3483    -0.02216    0.58369
C                          -3.45541    1.2047     0.38385
C                          -2.69915    0.00981    0.2855
C                          -3.4293    -1.20353    0.35024
C                          -2.75399    2.46       0.32079
C                          -1.28834    0.02741    0.12577
C                          -0.6173     1.28025    0.06539
C                          -1.40007    2.47544    0.16956
C                           0.79348    1.29778   -0.09855
C                           1.49093    0.06222   -0.20019
C                           0.82042   -1.19065   -0.13601
C                          -0.59037   -1.20821    0.02896
C                          -1.34702   -2.42248    0.09881
C                          -2.70079   -2.44097    0.25126
H                          -0.83753   -3.37458    0.02817
H                          -0.9114     3.44008    0.12667
C                           2.90006    0.08012   -0.37342
C                           3.65477   -1.11439   -0.48371
C                           3.6295     1.29358   -0.44637
N                           4.98228   -1.08803   -0.65722
N                           4.95678    1.3008     -0.6212
N                          -4.76022   -1.21023    0.4986
N                          -4.78657    1.17953    0.52849
C                           5.54325    0.11332   -0.72242
C                           2.95534   -2.36989   -0.40767
C                           1.60297   -2.38569   -0.2426
H                           1.1153    -3.35047   -0.1924
C                           1.55032    2.51206   -0.16767
H                           1.04191    3.46404   -0.08821
C                           2.90266    2.53079   -0.33183
C                           7.05481    0.14079   -0.95214
C                           7.91571    0.39052    0.31626
C                          -6.86989   -0.0492     0.74025
C                          -7.58946   -0.19611   -0.62588
F                           9.22127    0.42466   -0.02556
F                           7.46056   -1.02182   -1.50256
F                           7.35094    1.148      -1.80515
F                           7.56532    1.5694     0.87299
F                          -7.22979   -1.09093    1.51978
F                          -7.06629    0.70809   -1.48532
F                          -7.35317   -1.43537   -1.10041
F                          -7.29402    1.09411    1.32027
```

```
Br                             -3.63864   -4.10255    0.33896
Br                              3.92912   -4.00703   -0.54776
Br                              3.84036    4.19246   -0.41931
Br                             -3.72809    4.09743    0.45523
F                              -8.92619   -0.00845   -0.6047
F                               7.70881   -0.60545    1.20381
```

Compound 3

```
Charge =   0 Multiplicity = 1
C                              -5.3483    -0.02216    0.58369
C                              -3.45541    1.2047      0.38385
C                              -2.69915    0.00981     0.2855
C                              -3.4293    -1.20353     0.35024
C                              -2.75399    2.46         0.32079
C                              -1.28834    0.02741     0.12577
C                              -0.6173     1.28025     0.06539
C                              -1.40007    2.47544     0.16956
C                               0.79348    1.29778    -0.09855
C                               1.49093    0.06222    -0.20019
C                               0.82042   -1.19065    -0.13601
C                              -0.59037   -1.20821     0.02896
C                              -1.34702   -2.42248     0.09881
C                              -2.70079   -2.44097     0.25126
H                              -0.83753   -3.37458     0.02817
H                              -0.9114     3.44008     0.12667
C                               2.90006    0.08012    -0.37342
C                               3.65477   -1.11439    -0.48371
C                               3.6295     1.29358    -0.44637
N                               4.98228   -1.08803    -0.65722
N                               4.95678    1.3008     -0.6212
N                              -4.76022   -1.21023     0.4986
N                              -4.78657    1.17953     0.52849
C                               5.54325    0.11332    -0.72242
C                               2.95534   -2.36989    -0.40767
C                               1.60297   -2.38569    -0.2426
H                               1.1153    -3.35047    -0.1924
C                               1.55032    2.51206    -0.16767
H                               1.04191    3.46404    -0.08821
C                               2.90266    2.53079    -0.33183
C                               7.05481    0.14079    -0.95214
C                               7.91571    0.39052     0.31626
C                               7.80855   -0.66387     1.44001
C                              -6.86989   -0.0492      0.74025
C                              -7.58946   -0.19611    -0.62588
C                              -9.123      0.01918    -0.60158
F                               8.63165   -0.32814     2.43576
F                               6.55564   -0.69755     1.91898
F                               8.13639   -1.87709     1.00011
F                               9.20778    0.44092    -0.06829
F                               7.46056   -1.02182    -1.50256
F                               7.35094    1.148      -1.80515
F                               7.56623    1.58102     0.8459
F                              -7.22979   -1.09093     1.51978
F                              -9.69133   -0.74213     0.33669
F                              -9.41651    1.29768    -0.36354
F                              -9.62612   -0.3202     -1.79248
F                              -7.06629    0.70809    -1.48532
F                              -7.35317   -1.43537    -1.10041
F                              -7.29402    1.09411     1.32027
Br                             -3.63864   -4.10255     0.33896
Br                              3.92912   -4.00703    -0.54776
Br                              3.84036    4.19246    -0.41931
Br                             -3.72809    4.09743     0.45523
```

Compound 4

```
Charge =   0 Multiplicity = 1
C                              -5.35364   -0.02645    0.58033
C                              -3.46378    1.20166    0.38317
```

4

```
C                         -2.70133    0.00776    0.2849
C                         -3.43576   -1.20591    0.3491
C                         -2.7551     2.45058    0.31961
C                         -1.29046    0.0265     0.12678
C                         -0.62093    1.28042    0.06707
C                         -1.39984    2.47402    0.16935
C                          0.79257    1.2991    -0.09624
C                          1.49048    0.06354   -0.19766
C                          0.82155   -1.19041   -0.13359
C                         -0.592     -1.20912    0.03037
C                         -1.34288   -2.42285    0.0981
C                         -2.69815   -2.4356     0.2497
H                         -0.83526   -3.37612    0.02655
H                         -0.91469    3.44066    0.12563
C                          2.89957    0.08254   -0.37027
C                          3.6605    -1.11101   -0.48026
C                          3.63315    1.29634   -0.44358
N                          4.98652   -1.0838    -0.65341
N                          4.95906    1.30494   -0.61755
N                         -4.76541   -1.214      0.49547
N                         -4.79351    1.17564    0.52646
C                          5.54566    0.118     -0.71879
C                          2.95398   -2.36011   -0.40213
C                          1.60029   -2.38387   -0.23784
H                          1.11611   -3.35062   -0.18663
C                          1.54356    2.51286   -0.16406
H                          1.03689    3.46598   -0.08431
C                          2.89732    2.52583   -0.32818
C                          7.05711    0.14615   -0.94551
C                          7.91649    0.38646    0.32544
C                          7.80552   -0.67245    1.44455
C                         -6.875     -0.05421    0.73356
C                         -7.59412   -0.19456   -0.63332
C                         -9.12807    0.01724   -0.60856
F                          6.55567   -0.70042    1.92971
F                          8.1239    -1.88628    0.99796
F                          9.21017    0.43443   -0.05613
F                          7.46513   -1.01323   -1.50253
F                          7.35848    1.15855   -1.79127
F                          7.57131    1.57573    0.86109
F                         -7.23891   -1.09952    1.50741
F                         -9.42532    1.29355   -0.36218
F                         -9.63019   -0.31481   -1.80233
F                         -7.0743     0.71536   -1.48856
F                         -7.35643   -1.43094   -1.11547
F                         -7.30227    1.08644    1.31799
Br                        -3.62624   -4.06233    0.33081
Br                         3.92005   -3.96146   -0.53246
Br                         3.8254     4.15242   -0.41099
Br                        -3.72148    4.0521     0.44494
C                         -9.78388   -0.86927    0.46644
C                          8.76342   -0.29753    2.59062
F                         -9.53607   -0.35224    1.68864
F                         -9.27338   -2.1169     0.39366
F                        -11.1171    -0.91579    0.25939
F                          8.63801   -1.19301    3.59306
F                          8.4575     0.93536    3.04767
F                         10.03447   -0.30627    2.1358
```

Compound 5

Charge = 0 Multiplicity = 1
```
C                         -5.25729    0.07168    0.5684
C                         -3.36878    1.29371    0.32914
C                         -2.61814    0.09812    0.17512
C                         -3.3575    -1.11265    0.23717
C                         -2.65506    2.53983    0.26803
C                         -1.21356    0.11262   -0.0318
C                         -0.53845    1.36381   -0.08552
```

5

```
C                    -1.30582    2.55904    0.07038
C                     0.86919    1.37827   -0.29378
C                     1.55593    0.14133   -0.4435
C                     0.88105   -1.10986   -0.38836
C                    -0.52675   -1.12437   -0.18032
C                    -1.28284   -2.33508   -0.11633
C                    -2.63219   -2.34375    0.08156
H                    -0.78415   -3.28922   -0.22799
H                    -0.81637    3.5237     0.03164
C                     2.95982    0.15602   -0.6547
C                     3.70997   -1.03924   -0.81147
C                     3.69877    1.36696   -0.72041
N                     5.03185   -1.01598   -1.0138
N                     5.0204     1.37176   -0.92448
N                    -4.68091   -1.11674    0.43274
N                    -4.69232    1.27158    0.52186
C                     5.59698    0.1838    -1.0631
C                     2.99713   -2.28551   -0.74606
C                     1.64841   -2.30497   -0.54453
H                     1.15938   -3.26975   -0.50359
C                     1.62516    2.58909   -0.35868
H                     1.12674    3.54314   -0.24507
C                     2.97381    2.59795   -0.56078
C                     7.10606    0.20643   -1.30291
C                     7.97462    0.37787   -0.02083
C                     7.75445   -0.67907    1.08795
C                    -6.77128    0.04943    0.78392
C                    -7.5455    -0.06666   -0.55467
C                    -9.07733    0.2027    -0.53121
F                     6.52918   -0.47082    1.62657
F                     7.7993    -1.91592    0.55866
F                     9.27094    0.33347   -0.40011
F                     7.49943   -0.92369   -1.92346
F                     7.41703    1.25896   -2.09418
F                     7.71343    1.59229    0.50383
F                    -7.10672   -1.01469    1.54915
F                    -9.28915    1.50341   -0.25432
F                    -9.52242   -0.05536   -1.78113
F                    -7.02547    0.83967   -1.41616
F                    -7.34465   -1.30143   -1.05619
F                    -7.16617    1.17746    1.41032
Br                   -3.56814   -3.96632    0.15508
Br                    3.94733   -3.8893    -0.94369
Br                    3.90949    4.22051   -0.63647
Br                   -3.60572    4.14356    0.46393
C                    -9.9413    -0.63578    0.44009
C                     8.78161   -0.63599    2.24902
F                    -9.72555   -0.26261    1.70291
F                    -9.67231   -1.93649    0.3124
F                     8.37429   -1.46875    3.21119
F                     9.9844    -1.02558    1.82721
C                    -11.42691  -0.40198    0.10858
C                     8.88739    0.78404    2.83547
F                     9.55725    0.73848    4.00667
F                     7.64852    1.27799    3.04455
F                    -11.68546   0.92303    0.1113
F                    -11.70143  -0.91153   -1.11105
C                    -12.30444  -1.09839    1.16526
C                     9.64225    1.69258    1.84737
F                    -13.60446  -0.97467    0.82301
F                    -12.09957  -0.5241     2.36971
F                    -11.97854  -2.40689    1.22935
F                     10.15107   0.9436     0.84606
F                     8.79093    2.60762    1.33702
F                     10.64647   2.32298    2.49284
```

with B3PW91/6-311+g(d,p)
Compound **1**

```
Charge =   0 Multiplicity = 1
 C                     -5.48956    0.          0.03126
 C                     -3.57303    1.20374     0.01543
 C                     -2.81995    0.          0.01299
 C                     -3.57304   -1.20375     0.01534
 C                     -2.84497    2.44315     0.00989
 C                     -1.4001     0.          0.00665
 C                     -0.71151    1.24487     0.003
 C                     -1.48129    2.44874     0.00461
 C                      0.71151    1.24487    -0.00304
 C                      1.4001     0.00001    -0.00668
 C                      0.71151   -1.24486    -0.00301
 C                     -0.7115    -1.24486     0.00296
 C                     -1.48128   -2.44874     0.00446
 C                     -2.84495   -2.44316     0.0097
 H                     -0.98162   -3.40891     0.00075
 H                     -0.98163    3.40892     0.00097
 C                      2.81995    0.00001    -0.01301
 C                      3.57304   -1.20374    -0.01535
 C                      3.57303    1.20375    -0.01545
 N                      4.91064   -1.19485    -0.02276
 N                      4.91064    1.19485    -0.02287
 N                     -4.91063   -1.19486     0.02279
 N                     -4.91064    1.19484     0.02289
 C                      5.48956    0.00002    -0.03121
 C                      2.84496   -2.44315    -0.00973
 C                      1.48129   -2.44874    -0.00451
 H                      0.98163   -3.40891    -0.00081
 C                      1.48128    2.44875    -0.00465
 H                      0.98162    3.40892    -0.00103
 C                      2.84496    2.44316    -0.00991
 C                      7.0157    -0.00001     0.01016
 C                     -7.0157     0.         -0.01004
 F                      7.5172    -1.08362    -0.59009
 F                      7.51723    1.08369    -0.58991
 F                     -7.51719   -1.08372     0.59002
 F                     -7.5172     1.08358     0.59024
 Br                    -3.79826   -4.0577      0.01048
 Br                     3.79827   -4.05769    -0.01052
 Br                     3.79826    4.0577     -0.01089
 Br                    -3.79827    4.05769     0.01085
 F                     -7.43511    0.00011    -1.28864
 F                      7.43506   -0.00012     1.28876
```

Compound 2

```
Charge =   0 Multiplicity = 1
 C                      5.47471   -0.04436     0.40026
 C                      3.55421   -1.23222     0.25109
 C                      2.81243   -0.02245     0.20325
 C                      3.57306    1.17543     0.25903
 C                      2.81872   -2.46583     0.19306
 C                      1.39634   -0.0111      0.10091
 C                      0.69987   -1.25052     0.04778
 C                      1.45835   -2.4604      0.09711
 C                     -0.71951   -1.23926    -0.05394
 C                     -1.39637    0.01114    -0.10108
 C                     -0.69989    1.25056    -0.048
 C                      0.71948    1.2393      0.05376
 C                      1.49684    2.43704     0.10894
 C                      2.857      2.42072     0.20636
 H                      1.00616    3.40116     0.07227
 H                      0.95257   -3.41649     0.05681
 C                     -2.81246    0.02249    -0.20337
 C                     -3.55425    1.23226    -0.25125
 C                     -3.57308   -1.17539    -0.25905
 N                     -4.88874    1.23437    -0.34549
 N                     -4.90691   -1.15552    -0.35606
 N                      4.90686    1.15556     0.35614
```

```
N                4.88871   -1.23433    0.34541
C               -5.47476    0.04438   -0.40021
C               -2.81874    2.46587   -0.19336
C               -1.45837    2.46044   -0.09742
H               -0.95259    3.41653   -0.0572
C               -1.49687   -2.43699   -0.10907
H               -1.00619   -3.40112   -0.07241
C               -2.85704   -2.42068   -0.2064
C               -6.99908    0.05112   -0.49882
C               -7.69386   -0.05403    0.87861
C                6.99901   -0.05116    0.49917
C                7.69404    0.05383   -0.87813
F               -9.01909    0.01256    0.73502
F               -7.4241     1.19447   -1.07605
F               -7.41973   -0.99448   -1.24408
F               -7.38203   -1.21213    1.46826
F                7.41959    0.99454    1.24439
F                7.29562   -0.94957   -1.66938
F                7.38242    1.21199   -1.4678
F                7.42385   -1.19444    1.07663
Br               3.82068    4.02746    0.27358
Br              -3.75693    4.08787   -0.25287
Br              -3.82071   -4.02743   -0.27358
Br               3.75692   -4.08783    0.25238
F                9.01926   -0.01288   -0.7343
F               -7.2954     0.94944    1.66979
```

Compound 3

```
Charge =   0 Multiplicity = 1
C               -5.35364   -0.02645    0.58033
C               -3.46378    1.20166    0.38317
C               -2.70133    0.00776    0.2849
C               -3.43576   -1.20591    0.3491
C               -2.7551     2.45058    0.31961
C               -1.29046    0.0265     0.12678
C               -0.62093    1.28042    0.06707
C               -1.39984    2.47402    0.16935
C                0.79257    1.2991    -0.09624
C                1.49048    0.06354   -0.19766
C                0.82155   -1.19041   -0.13359
C               -0.592     -1.20912    0.03037
C               -1.34288   -2.42285    0.0981
C               -2.69815   -2.4356     0.2497
H               -0.83526   -3.37612    0.02655
H               -0.91469    3.44066    0.12563
C                2.89957    0.08254   -0.37027
C                3.6605    -1.11101   -0.48026
C                3.63315    1.29634   -0.44358
N                4.98652   -1.0838    -0.65341
N                4.95906    1.30494   -0.61755
N               -4.76541   -1.214      0.49547
N               -4.79351    1.17564    0.52646
C                5.54566    0.118     -0.71879
C                2.95398   -2.36011   -0.40213
C                1.60029   -2.38387   -0.23784
H                1.11611   -3.35062   -0.18663
C                1.54356    2.51286   -0.16406
H                1.03689    3.46598   -0.08431
C                2.89732    2.52583   -0.32818
C                7.05711    0.14615   -0.94551
C                7.91649    0.38646    0.32544
C                7.80552   -0.67245    1.44455
C               -6.875     -0.05421    0.73356
C               -7.59412   -0.19456   -0.63332
C               -9.12807    0.01724   -0.60856
F                8.63615   -0.34734    2.43835
F                6.55567   -0.70042    1.92971
F                8.1239    -1.88628    0.99796
```

8

```
F                   9.21017    0.43443   -0.05613
F                   7.46513   -1.01323   -1.50253
F                   7.35848    1.15855   -1.79127
F                   7.57131    1.57573    0.86109
F                  -7.23891   -1.09952    1.50741
F                  -9.69674   -0.75148    0.32361
F                  -9.42532    1.29355   -0.36218
F                  -9.63019   -0.31481   -1.80233
F                  -7.0743     0.71536   -1.48856
F                  -7.35643   -1.43094   -1.11547
F                  -7.30227    1.08644    1.31799
Br                 -3.62624   -4.06233    0.33081
Br                  3.92005   -3.96146   -0.53246
Br                  3.8254     4.15242   -0.41099
Br                 -3.72148    4.0521     0.44494
```

Compound 4

```
Charge =   0 Multiplicity = 1
C                  -5.25729    0.07168    0.5684
C                  -3.36878    1.29371    0.32914
C                  -2.61814    0.09812    0.17512
C                  -3.3575    -1.11265    0.23717
C                  -2.65506    2.53983    0.26803
C                  -1.21356    0.11262   -0.0318
C                  -0.53845    1.36381   -0.08552
C                  -1.30582    2.55904    0.07038
C                   0.86919    1.37827   -0.29378
C                   1.55593    0.14133   -0.4435
C                   0.88105   -1.10986   -0.38836
C                  -0.52675   -1.12437   -0.18032
C                  -1.28284   -2.33508   -0.11633
C                  -2.63219   -2.34375    0.08156
H                  -0.78415   -3.28922   -0.22799
H                  -0.81637    3.5237     0.03164
C                   2.95982    0.15602   -0.6547
C                   3.70997   -1.03924   -0.81147
C                   3.69877    1.36696   -0.72041
N                   5.03185   -1.01598   -1.0138
N                   5.0204     1.37176   -0.92448
N                  -4.68091   -1.11674    0.43274
N                  -4.69232    1.27158    0.52186
C                   5.59698    0.1838    -1.0631
C                   2.99713   -2.28551   -0.74606
C                   1.64841   -2.30497   -0.54453
H                   1.15938   -3.26975   -0.50359
C                   1.62516    2.58909   -0.35868
H                   1.12674    3.54314   -0.24507
C                   2.97381    2.59795   -0.56078
C                   7.10606    0.20643   -1.30291
C                   7.97462    0.37787   -0.02083
C                   7.75445   -0.67907    1.08795
C                  -6.77128    0.04943    0.78392
C                  -7.5455    -0.06666   -0.55467
C                  -9.07733    0.2027    -0.53121
F                   6.52918   -0.47082    1.62657
F                   7.7993    -1.91592    0.55866
F                   9.27094    0.33347   -0.40011
F                   7.49943   -0.92369   -1.92346
F                   7.41703    1.25896   -2.09418
F                   7.71343    1.59229    0.50383
F                  -7.10672   -1.01469    1.54915
F                  -9.28915    1.50341   -0.25432
F                  -9.52242   -0.05536   -1.78113
F                  -7.02547    0.83967   -1.41616
F                  -7.34465   -1.30143   -1.05619
F                  -7.16617    1.17746    1.41032
Br                 -3.56814   -3.96632    0.15508
Br                  3.94733   -3.8893    -0.94369
```

9

```
Br                           3.90949    4.22051   -0.63647
Br                          -3.60572    4.14356    0.46393
C                           -9.9413    -0.63578    0.44009
C                            8.78161   -0.63599    2.24902
F                           -9.72555   -0.26261    1.70291
F                           -9.67231   -1.93649    0.3124
F                          -11.22989   -0.43298    0.15255
F                            8.37429   -1.46875    3.21119
F                            8.87331    0.59502    2.75741
F                            9.9844    -1.02558    1.82721
```

Compound 5

```
Charge =   0 Multiplicity = 1
C                            4.83781   -0.33458    0.33451
C                            2.8701    -1.35894   -0.10918
C                            2.21783   -0.09767   -0.11323
C                            3.04432    1.03066    0.13064
C                            2.06561   -2.52454   -0.35485
C                            0.82389    0.02828   -0.35071
C                            0.05762   -1.14614   -0.59174
C                            0.72597   -2.40914   -0.5829
C                           -1.33898   -1.01984   -0.83287
C                           -1.92456    0.27687   -0.8234
C                           -1.15876    1.45105   -0.58078
C                            0.2385     1.325     -0.3422
C                            1.08151    2.45187   -0.09426
C                            2.42051    2.32548    0.13194
H                            0.66033    3.44902   -0.08186
H                            0.16567   -3.31781   -0.76193
C                           -3.31793    0.40317   -1.06345
C                           -3.9709     1.66363   -1.06463
C                           -4.14316   -0.72405   -1.31632
N                           -5.28561    1.77359   -1.28685
N                           -5.45296   -0.59459   -1.54877
N                            4.35722    0.90306    0.35223
N                            4.185     -1.46854    0.11191
C                           -5.93804    0.6415    -1.51593
C                           -3.16728    2.8289    -0.81524
C                           -1.82753    2.7137    -0.58718
H                           -1.26778    3.62221   -0.4057
C                           -2.18162   -2.14629   -1.08531
H                           -1.76074   -3.14357   -1.09701
C                           -3.51937   -2.01905   -1.31757
C                           -7.43348    0.76262   -1.81025
C                           -8.40306    0.18421   -0.73394
C                           -8.35628    0.88671    0.64753
C                            6.34198   -0.46109    0.58304
C                            7.16266   -0.24713   -0.71527
C                            8.68364   -0.59739   -0.6843
F                           -7.06289    1.00593    1.0385
F                           -8.86838    2.11886    0.49777
F                           -9.65531    0.31723   -1.21704
F                           -7.77029    2.05294   -2.00157
F                           -7.7046     0.0727    -2.94536
F                           -8.13571   -1.12793   -0.56893
F                            6.73269    0.46951    1.48286
F                            8.81113   -1.92745   -0.52976
F                            9.16501   -0.24928   -1.90064
F                            6.63088   -1.04189   -1.67422
F                            7.03044    1.03656   -1.10123
F                            6.62842   -1.68577    1.0717
Br                           3.47576    3.84148    0.45206
Br                          -3.98719    4.51473   -0.80867
Br                          -4.57504   -3.5339    -1.6419
Br                           2.88483   -4.21062   -0.35705
C                            9.54712    0.10896    0.39621
C                           -9.16595    0.16572    1.78848
F                            9.31332   -0.49606    1.58073
```

10

```
F                      9.19108    1.40551    0.47939
F                     -9.76348    1.13108    2.5162
F                    -10.12374   -0.6128     1.24468
C                     11.07478    0.0556     0.10784
C                     -8.38431   -0.68596    2.83567
F                     -9.31762   -1.12972    3.70624
F                     -7.52687    0.12096    3.49154
F                     11.41294   -1.17914   -0.31769
F                     11.36204    0.95301   -0.85359
C                     11.96483    0.38423    1.33649
C                     -7.60071   -1.93526    2.36835
F                     13.22425    0.54449    0.92364
F                     11.92887   -0.60892    2.22455
F                     11.55679    1.5128     1.92291
F                     -8.39753   -2.76594    1.69683
F                     -6.56415   -1.59539    1.59864
F                     -7.13358   -2.56572    3.44948
```

S3. X-Ray Crystal Structure Determinations

Crystal data and details of the structure determinations are listed in Table S1. Full shells of intensity data were collected at low temperature (110 K) with a Agilent Technologies Supernova-E CCD diffractometer (Cu-K_a radiation, l = 1.54184 Å, microfocus tube, multilayer mirror optics). Data were corrected for air and detector absorption, Lorentz and polarization effects;[S4] absorption by the crystal was treated numerically (Gaussian grid)[S4] (compound **2**) or analytically[S4,S5] (compound **3**). The structures were solved by the charge flip procedure[S6] and refined by full-matrix least squares methods based on F^2 against all unique reflections.[S7] All non-hydrogen atoms were given anisotropic displacement parameters. Hydrogen atoms were placed at calculated positions and refined with a riding model.[S7] CCDC 911239 and 911240 contain the supplementary crystallographic data for this paper. These data can be obtained free of charge from The Cambridge Crystallographic Data Centre via www.ccdc.cam.ac.uk/data_request/cif.

Table S1. Details of the crystal structure determinations of **2** and **3**.

	2	3
formula	$C_{26}H_4Br_4F_{10}N_4$	$C_{28}H_4Br_4F_{14}N_4$
M_r	881.97	981.99
crystal system	triclinic	triclinic
space group	P -1	P -1
a /Å	5.0066(3)	4.9853(2)
b /Å	9.7801(7)	10.1228(5)
c /Å	13.0065(6)	13.8975(6)
α /°	91.231(5)	103.981(4)
β /°	95.117(4)	95.353(4)
γ /°	90.984(5)	91.166(4)
V /Å^3	634.06(6)	676.93(6)
Z	1	1
F_{000}	418	466
d_c /Mg·m^{-3}	2.310	2.409
μ /mm^{-1}	8.708	8.477
max., min. transmission factors	0.819, 0.416	0.868, 0.348
θ range /°	4.5 to 71.9	4.5 to 72.3
index ranges (indep. set) h,k,l	-6 ... 6, -11 ... 12, -16 ... 15	-6 ... 6, -12 ... 12, -17 ... 17
reflections measured	19590	34044
unique [R_{int}]	2426 [0.0825]	2596 [0.1121]
observed [$I{\geq}2\sigma(I)$]	2069	2389
parameters refined	199	226
GooF on F^2	1.112	1.127
R indices [$F>4\sigma(F)$] $R(F)$, $wR(F^2)$	0.0347, 0.0871	0.0440, 0.1208
R indices (all data) $R(F)$, $wR(F^2)$	0.0444, 0.0914	0.0475, 0.1272
largest residual peaks /e·Å^{-3}	0.957, -0.684	1.600, -1.328

*S4. Comparison of experimental and computed bond lengths and angles of compound **2**:*

bond lengths			bond angles		
	X-Ray [Å]	DFT [Å]		X-Ray [°]	DFT [°]
Br(1)-C(2)	1.875(3)	1.875	C(21)-N(1)-C(1)	115.7(3)	116.2
Br(2)-C(8)	1.874(4)	1.875	C(21)-N(2)-C(7)	114.9(3)	116.2
N(1)-C(21)	1.327(5)	1.328	N(1)-C(1)-C(6)	121.2(4)	121.3
N(1)-C(1)	1.347(5)	1.337	N(1)-C(1)-C(2)	120.7(3)	120.8
N(2)-C(21)	1.337(5)	1.328	C(6)-C(1)-C(2)	118.1(3)	117.6
N(2)-C(7)	1.348(5)	1.338	C(3)-C(2)-C(1)	120.9(3)	120.7
C(1)-C(6)	1.419(5)	1.420	C(3)-C(2)-Br(1)	120.5(3)	120.3
C(1)-C(2)	1.433(6)	1.437	C(1)-C(2)-Br(1)	118.7(3)	119.0
C(2)-C(3)	1.362(5)	1.364	C(2)-C(3)-C(4)	121.9(4)	122.4
C(3)-C(4)	1.434(5)	1.429	C(5)-C(4)-C(10)	118.8(3)	118.9
C(4)-C(5)	1.418(6)	1.423	C(10)-C(4)-C(3)	122.5(4)	122.6
C(4)-C(10)	1.420(5)	1.423	C(5)-C(4)-C(3)	118.7(4)	118.5
C(5)-C(6)	1.427(5)	1.420	C(7)-C(6)-C(1)	116.8(3)	115.9
C(6)-C(7)	1.410(6)	1.420	N(1)-C(21)-N(2)	129.3(4)	128.3
C(21)-C(22)	1.526(5)	1.528	N(1)-C(21)-C(22)	115.9(3)	115.6

*S.5 Meting points of compounds **1 – 5** obtained from DSC scans*

Compound	**Melting point [C°]** (DSC 35-800°C @ 10° K/min N$_2$)
1	512.27
2	455.74
3	405.63
4	387.08
5	335.77

All compounds melt without composition (which sets in at temperatures above the meting point). As an example the DSC/TGA trace of **1** is displayed below (Figure S1). Those of **2-5** were found to be very similar.

13
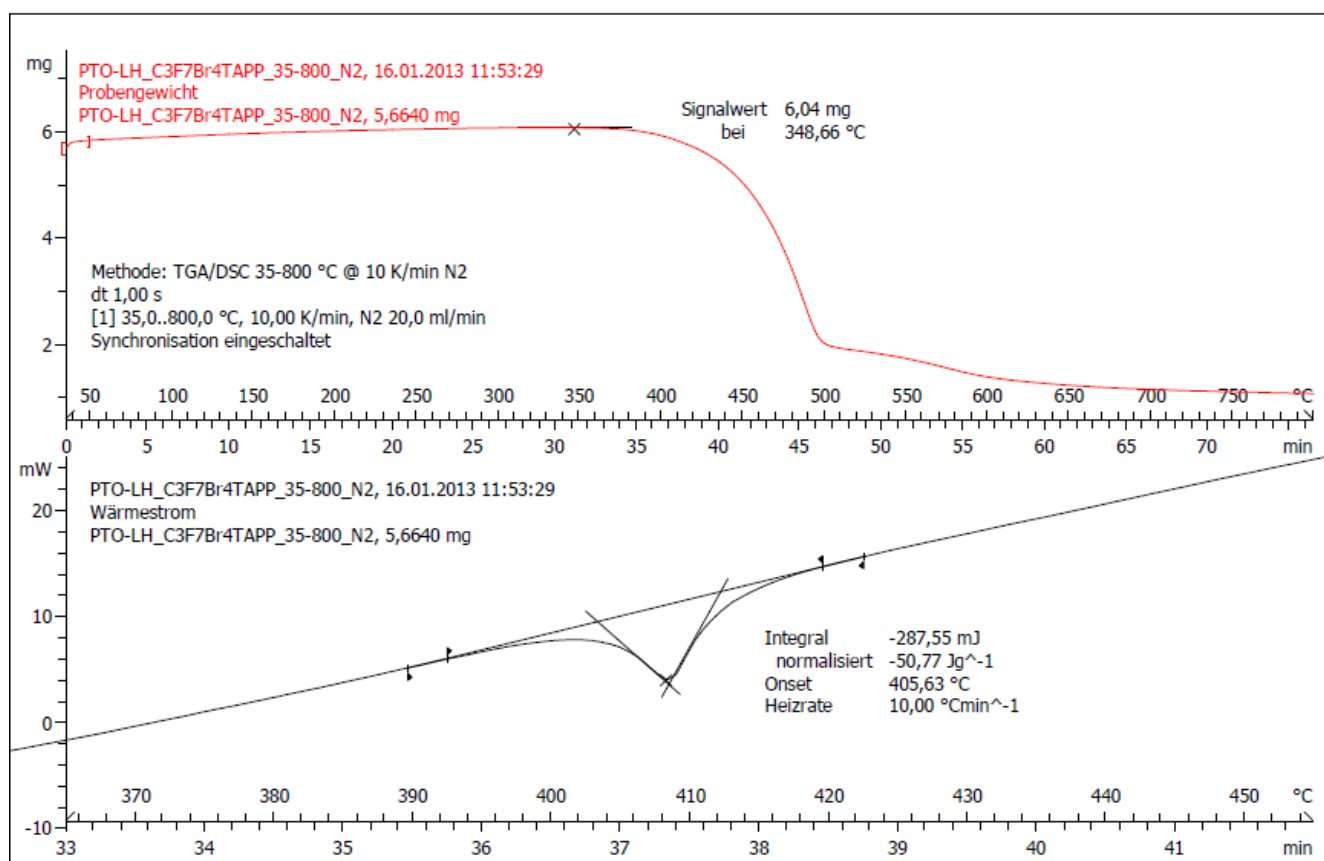
Figure S1. TGA/DSC trace of **1**.

S6. Detailed description of the TFT fabrication

S6.1. TFTs fabricated by vacuum deposition

<u>TFTs with thick gate dielectric and vacuum-deposited semiconductor on silicon substrates:</u>

A heavily doped silicon wafer was used as the substrate and common gate electrode. The silicon surface was thermally oxidized in dry oxygen to obtain a 100-nm-thick layer of silicon dioxide. Onto the SiO_2 surface, an 8-nm-thick layer of aluminum oxide was deposited by atomic layer deposition at a substrate temperature of 250 °C. The substrate was then immersed into a 2-propanol solution of tetradecylphosphonic acid (PCI Synthesis) for about 1 hour to allow a 1.7-nm-thick self-assembled monolayer (SAM) to form. Thus, the gate dielectric is a combination of 100-nm-thick SiO_2, 8-nm-thick AlO_x and a 1.7-nm-thick SAM. Onto the gate dielectric, a semiconductor layer with a thickness of 25 to 30 nm was deposited

14

by sublimation in vacuum. Finally, 30-nm-thick Au source and drain contacts were deposited on top of the semiconductor by thermal evaporation in vacuum through a shadow mask.

TFTs with thin gate dielectric and vacuum-deposited semiconductor on silicon substrates:

A heavily doped silicon wafer was used as the substrate. A 20-nm-thick layer of aluminum was deposited as the gate electrode. The Al surface was oxidized by exposing it for about 30 seconds to an oxygen plasma in a reactive ion etcher to produce an aluminum oxide layer with a thickness of about 3.6 nm. The substrate was then immersed into a 2-propanol solution of tetradecylphosphonic acid for about 1 hour to allow a 1.7-nm-thick SAM to form. Thus, the gate dielectric is a combination of 3.6-nm-thick AlO_x and a 1.7-nm-thick SAM. A semiconductor layer with a thickness of 25 to 30 nm was deposited by sublimation in vacuum, followed by the deposition of the Au source and drain contacts through a shadow mask

Complementary inverters and ring oscillators on flexible substrates:

125-µm-thick polyethylene naphthalate (PEN) film was used as the substrate. Patterned gate electrodes were defined by depositing 20-nm-thick aluminum by thermal evaporation through a shadow mask directly onto the PEN. The gate dielectric was a combination of 3.6-nm-thick AlO_x (grown by plasma oxidation) and a 1.7-nm-thick SAM (obtained from solution, as described above). A semiconductor layer with a thickness of 25 nm was deposited by sublimation in vacuum, followed by the deposition of the Au source and drain contacts through a shadow mask.

All electrical measurements were performed on a probe station in ambient air.

S6.2. AFM pictures of device surfaces that were prepared by vacuum deposition

Figure S2.   AFM pictures of OTFT Devices

with compound **1**

with compound **2**

with compound **3**

with compound **4**

with compound **5**
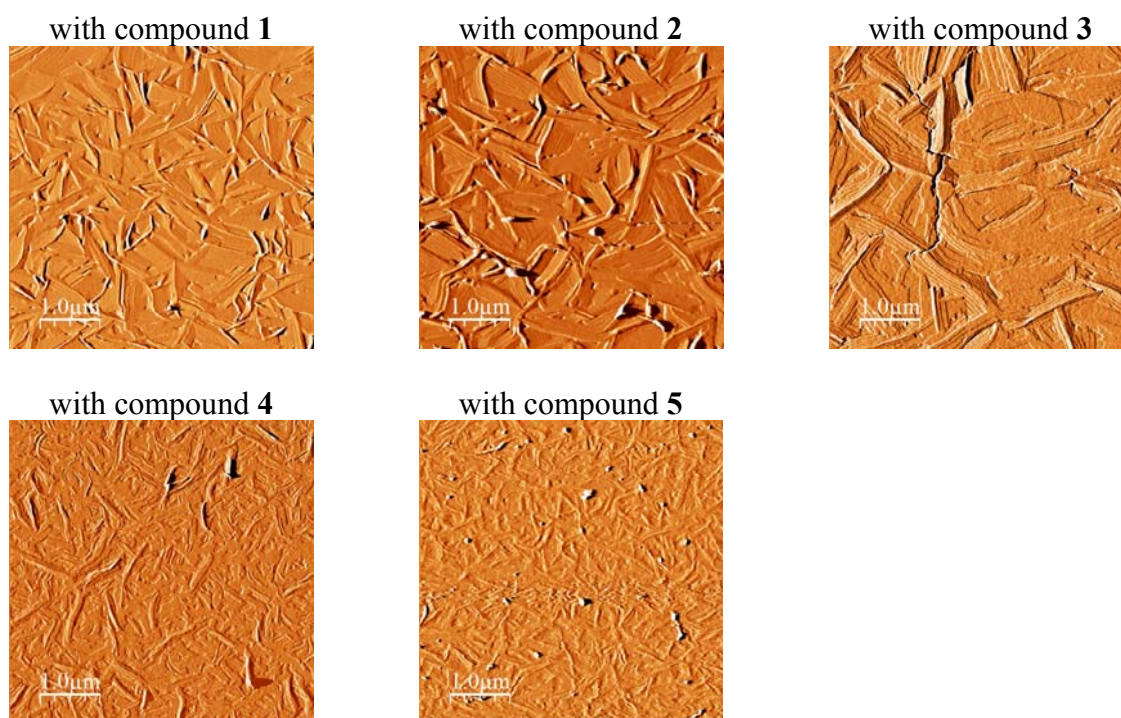
S6.3. TFTs fabricated by solution shearing

Highly doped n-type Si (100) wafers (< 0.02 Ω cm) with 100 nm SiO_2 as gate dielectric (capacitance per unit area $C_i = 34$ nF/cm^2) were used as substrates for thin-film deposition by solution shearing. These wafers were subsequently rinsed with toluene, acetone, isopropyl alcohol and finally treated for 5 minutes with UV/ozone before device manufacturing. TAPP **3** was stirred in o dichlorobenzene at 100 °C to fully solubilize at a concentration of about 2 mg/ml. The organic semiconductor thin films were deposited through solution shearing with an octadecyltriethoxysilane (OTES) functionalized Si wafer as shearing tool. Solution-sheared thin films were prepared at a shearing speed of 0.08 mm/s and a substrate and shearing tool temperature of 130 °C. Source and drain electrodes were patterned by evaporation of gold (30 nm) onto the thin films using shadow masks with a channel length (L) of 100 μm, and a channel width (W) of 200 μm at a pressure of 1 x 10^{-6} mbar and an evaporation rate of 1.8 nm min^{-1}.The TFT transfer and output characteristics were recorded either under ambient

16

conditions by using an Agilent 4155C semiconductor parametric analyser (Agilent Technologies, Inc., Santa Clara, CA) at 298 K. The electron charge carrier mobility μ_n was determined in the saturation regime from the slope of the plot of the square root of the drain-source current vs. the gate-source voltage.
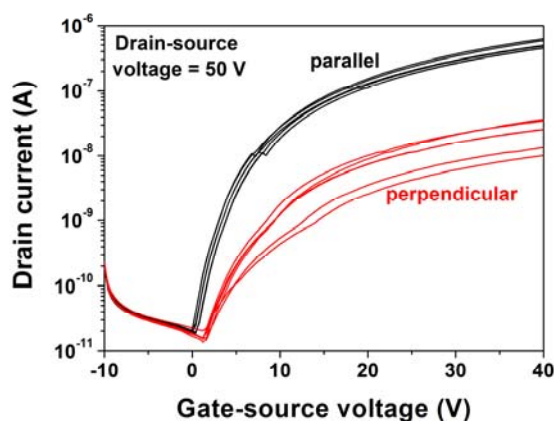

Figure S3. Transfer characteristics of each six TFTs of TAPP **3** in parallel (black) and perpendicular (red) orientation, respectively, with regard to the shearing direction.
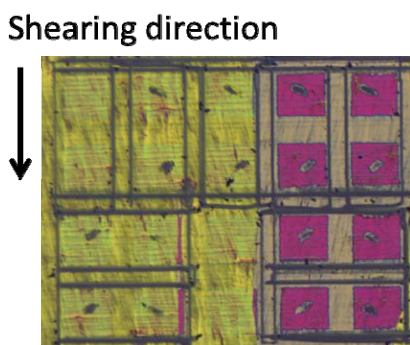

Figure S4. Optical microscopic image of TFT devices of TAPP **3** under cross-polarised light processed by solution shearing. The black arrow indicates the direction of shearing and equals a scale bar of 500 μm.

S7. References

[S1] (a) W. J. Hehre, R. Ditchfield, J. A. Pople, *J. Chem. Phys.* **1972**, 56, 2257; (b) J. A. Pople, *J. Chem. Phys.* **1975**, *62*, 2921; (c) M. M. Francl, W. J. Petro, W. J. Hehre, J. S. Binkley, M. S. Gordon, D. J. DeFrees, J. A. Pople, *J. Chem. Phys.* **1982**, *77*, 3654; (d) T. Clark, J. Chandrasekhar, G. W. Spitznagel, P. v. R. Schleyer, *J. Comp. Chem.* **1983**, *4*, 294.

[S2] Gaussian 09, Revision A.02, M. J. Frisch, G. W. Trucks, H. B. Schlegel, G. E. Scuseria, M. A. Robb, J. R. Cheeseman, G. Scalmani, V. Barone, B. Mennucci, G. A. Petersson, H. Nakatsuji, M. Caricato, X. Li, H. P. Hratchian, A. F. Izmaylov, J. Bloino, G. Zheng, J. L. Sonnenberg, M. Hada, M. Ehara, K. Toyota, R. Fukuda, J. Hasegawa, M. Ishida, T. Nakajima, Y. Honda, O. Kitao, H. Nakai, T. Vreven, J. A. Montgomery, Jr., J. E. Peralta, F. Ogliaro, M. Bearpark, J. J. Heyd, E. Brothers, K. N. Kudin, V. N. Staroverov, R. Kobayashi, J. Normand, K. Raghavachari, A. Rendell, J. C. Burant, S. S. Iyengar, J. Tomasi, M. Cossi, N. Rega, J. M. Millam, M. Klene, J. E. Knox, J. B. Cross, V. Bakken, C. Adamo, J. Jaramillo, R. Gomperts, R. E. Stratmann, O. Yazyev, A. J. Austin, R. Cammi, C. Pomelli, J. W. Ochterski, R. L. Martin, K. Morokuma, V. G. Zakrzewski, G. A. Voth, P. Salvador, J. J. Dannenberg, S. Dapprich, A. D. Daniels, O. Farkas, J. B. Foresman, J. V. Ortiz, J. Cioslowski, and D. J. Fox, Gaussian, Inc., Wallingford CT, **2009**.

[S3] (a) Y.-C. Chang, M.-Y. Kuo, C.-P. Chen, H. F. Lu, I. Chao, *J. Phys. Chem. C* **2010**, *114*, 11595; (b) J. C. Rienstra-Kiracofe, G. S. Tschumper, H. F. Schaefer III, S. Nandi, G. B. Ellison, *Chem. Rev.* **2002**, *102*, 231-282.

[S4] *CrysAlisPro*, Agilent Technologies UK Ltd., Oxford **2011**.

[S5] R. C. Clark, J. S. Reid, *Acta Cryst.* **1995**, *A51*, 887.

[S6] (a) L. Palatinus, *SUPERFLIP*, EPF Lausanne, Switzerland, **2007**; (b) L. Palatinus, G. Chapuis, *J. Appl. Cryst.* **2007**, 40, 786.

[S7] (a) G. M. Sheldrick, *SHELXL-97*, University of Göttingen, **1997**; (b) G. M. Sheldrick, *Acta Cryst.* **2008**, *A64*, 112.